SUPEREXCHANGE COUPLING IN FLUORIDES AND FLUORO-COMPLEXES OF ELEMENTS IN THE FIRST TRANSITION SERIES

By

S.S.I. Kaseno

This Thesis is Submitted in Partial Fulfillment of the Requirements for the Degree of Master of Science at the Department of Chemistry, University of Ottawa.

August, 1961

A.D. Westland
Assistant Professor of Chemistry
Research Supervisor.

S.S.I. Kaseno
Candidate.

PREFACE

Magnetic susceptibility measurements have been used by inorganic chemists principally for the determination of oxidation states and to a lesser extent for the determination of the stereochemistry of complexes. Very recently, investigation of the influence of temperature has been used for the estimation of bond parameters.

Of the various types of inorganic compounds, fluorides contain the most electrovalent bonds, hence these might be expected to conform most nearly to the simpler theory of magnetism and provide suitable systems for studies of the chemical bonding.

However, fluorides and fluoro complexes of the transition series frequently possess effective magnetic moments which are much lower than the predicted values, and which are strongly dependent upon temperature. The present thesis describes an attempt to discover the source or sources of those deviations among compounds formed by members of the first transition series.

The research was begun under the assumption that the principle cause of the magnetic anomalies resided in the fact that fluorides, like the extensively studied oxide systems, are rarely "magnetically dilute". Since this proved

to be true, it was of interest to determine whether the interactions between paramagnetic ions are of direct or indirect type. The behaviour of oxides (ferrites, etc.) has recently been ascribed to the latter type of interaction.

The principle aim of this thesis is to show that the information which can be obtained from the magnetic properties of fluorides is compatible with theories of indirect exchange and electronic configuration which have been applied to oxides.

Acknowledgment

This work was done under the direction of Dr. A.D. Westland, whose scientific guidance has been the mainstay of the investigation. For this and the many valuable discussions during the preparation of the thesis the author wishes to express her sincere gratitude.

The grant from the National Research Council of Canada is hereby gratefully acknowledged.

CONTENTS

LIST OF TABLES

LIST OF FIGURES

ABSTRACT

Theories of magnetism with special reference to the indirect exchange mechanism and ligand field theory are discussed.

The magnetic susceptibilities of VF_3, MnF_3, NiF_2-MgF_2, K_2NiF_4-K_2MgF_4, and K_3NiF_6-$K_{2.8}AlF_{5.8}$ were studied over a temperature range of 90° K to 300° K.

The effective magnetic moments of the paramagnetic ions increases as their concentration in the solid solutions decreases. This is explained as being due to the presence of indirect interactions between paramagnetic ions in the pure substance which are decreased by magnetic dilution. It was found that the moments are still dependent upon temperature even at infinite dilution. This behaviour is ascribed to the orbital contribution which is itself temperature dependent.

Evidence is adduced for the presence of Ni(III) ion impurities in the NiF_2-MgF_2 system when it is contaminated with traces of oxide.

INTRODUCTION

A. Theories of Magnetism

Magnetic effects are of two types, one arising from the motion of the electrons which are charged particles, and the other from the spin and orbital angular momentum of unpaired electrons. The former effect gives rise to the phenomenon of diamagnetism and the latter to that of paramagnetism. In most cases the effects of diamagnetism are small compared to those of paramagnetism, and it will be dealt with here only as a correction in paramagnetic measurements.

Ferromagnetism and antiferromagnetism are extensions of paramagnetism; they are the result of interactions between magnetic dipoles on neighbouring atoms. In a filled shell, both the spin and orbital angular momenta of the electrons cancel out to zero, and the system is left with only the diamagnetic effect. This is the reason that paramagnetism is found mainly in the transitional and lanthanide series.

If a substance is placed in a magnetic field of strength H, then the magnetic induction B, the field inside the specimen, is expressed as

$$\vec{B} = \vec{H} + 4\pi \vec{I}$$

where I is the intensity of magnetization, the degree of dipole alignment or charge polarization induced by the field. The strength of a magnetic field is expressed in "oersteds" or "gauss" is often used incorrectly in the same sense. A field has a strength of one oersted if a unit magnetic pole placed in it experiences a force of one dyne.

Quantitatively the most important chemical aspects of magnetism can be expressed as the magnetic susceptibility, either as the "volume susceptibility" κ , or the "gram susceptibility" χ

$$\kappa = I/H \quad \text{and} \quad \chi = \kappa/\rho$$

where ρ is the density of the material

Table I

Classes of Magnetic Behaviour

Class of magnetism	Sign of χ	Magnitude	Field Dependence
Diamagnetic	-ve	1×10^{-6} c.g.s.	Indep. of H
Paramagnetic	+ve	$1 \text{ to } 100 \times 10^{-6}$ c.g.s	Indep. of H
Ferromagnetic	+ve	10^{-2} to 10^{4} c.g.s	Dependent on H
Antiferromagnetic	+ve	$1 \text{ to } 100 \times 10^{-6}$ c.g.s	Often dependent on H

It is sometimes convenient to deal with "susceptibilities per mole" or per gram atom.

$$\chi_M = \chi \times \text{molecular weight}$$

$$\chi_A = \chi \times \text{atomic weight}$$

Although diamagnetic susceptibilities are usually small compared with the paramagnetic ones, in cases where the number of ligand atoms in a complex compound is very large, the diamagnetic contribution to the susceptibility may become quite considerable. This is particularly important for large organic molecule ligands.

The Classical Theory of Paramagnetism and Diamagnetism

A classical theory of paramagnetism was developed by Langevin[1] on the assumption that each atom is a little permanent magnet. These atomic magnets would tend to line up parallel to an applied magnetic field were they not prevented by the "temperature agitation". This influence becomes stronger with increasing temperature.

Langevin expressed the molar paramagnetism as

$$\chi_M = N \mu^2 / 3 kT \qquad [1]$$

where N is the Avogadro number, μ is the permanent moment, k is the Boltzmann constant, and T is the absolute temperature. A precise expression will also include a term for the relatively small diamagnetic part of the susceptibility. Expression [1] is applicable only for cases where molecular interactions are negligible. Paramagnetic susceptibility is inversely proportional

to the absolute temperature, provided that the density is kept constant. This is known as Curie's law[2] $\chi = \frac{C}{T}$, obtained experimentally before Langevin's theory. C is the Curie constant. The Curie law is approximately true in many instances, but the more accurate magnetic measurements become, the more are deviations from it discovered.

In diamagnetism, one considers the induced rather than the permanent magnetic moment of the atom. The magnetic moment resulting from orbital motion is proportional to the angular momentum. Suppose the molecule has no electronic angular momentum in the absence of the external fields; if now a magnetic field is applied, the electronic motion is modified, and an induced angular momentum is created. In general the diamagnetic susceptibility is independent of temperature.

Van Vleck[3] using quantum mechanics obtained the analogous expression for paramagnetism:

$$\chi_M = N \bar{\mu}^2/3kT + N \bar{\alpha} \qquad [2]$$

$N \bar{\alpha}$ is the combined temperature independent contribution of the high frequency elements of the paramagnetic moment and of the diamagnetic part. Equation [2] can also be expressed as

$$\chi_M = N \left[\frac{\beta^2 \bar{\mu}_\beta^2}{3kT} + \bar{\alpha} \right] \qquad [3]$$

where μ_β is the low frequency part of the magnetic moment expressed in Bohr magnetons. The Bohr magneton is a unit of

atomic magnetic moment whose magnitude is given by

$$\beta = eh/4\pi mc = 0.917 \times 10^{-20} \text{ erg oersted}^{-1}$$

Quantum Theory

In the previous section it was mentioned that in general the magnetic moment of an atom consists of the orbital contribution and the electron spin contribution. This can be expressed in vector notation as

$$\overline{\mu} = (\overrightarrow{L} + 2\overrightarrow{S})\ \beta$$

where $\overrightarrow{L}$ is the total orbital angular momentum and $\overrightarrow{S}$ the total spin angular momentum (in units of $\frac{h}{2\pi}$) of the set of electrons in the atom. In different normal states of the atom, the inclination of the orbital and spin contributions may be different. However, in most cases of "molecular" paramagnetism in contrast with "atomic" paramagnetism, the orbital contribution appears to be quenched out.

In most cases one deals with atoms which have more than one electron and the magnetic moment of those atoms will depend on the way the orbital angular and spin momenta of the atoms combine.

The most frequent type of coupling is "Russell-Saunders" coupling (LS coupling) in which all the orbital angular momenta ℓ of the electrons combine vectorially to give the resultant quantum number L. Similarly the angular momenta due

to the spin s couple together algebraically, to give the resultant S. Further the resultant angular momenta J, are obtained by different vectorial combinations of L and S

$$J = L + S,\ L + S - 1,\ L + S - 2, \text{-------}, /L-S/.$$

Although the LS Coupling, in which the interaction of the individual ℓ vectors and the s vectors is strong, is common to the majority of elements, in some cases the "spin-orbit" interaction of each electron is stronger. This may lead to the "j-j" coupling.

LS coupling applies very well for those atoms with $z \lesssim 30$, where z is the atomic number, at least up to the end of the first transitional series, and the j-j coupling for the heavy atoms such as those of the third transitional series. In evaluating $\bar{\mu}^2$ and α in equation [3] there are three cases for which different equations are required:

a) Multiplet intervals small compared to kT.

The high frequency elements of the paramagnetic moment are absent, and the paramagnetic susceptibility can be expressed by

$$\chi_M = \frac{N\beta^2}{3kT} [4S (S + 1) + L (L + 1)] \qquad [4]$$

In many crystalline compounds, the orbital contribution to the magnetic moment may be quenched out. This leads to the so-called "spin only" formula

$$\chi_M = \frac{N\beta^2}{3kT} [4S (S + 1)] \qquad [5]$$

Equation [5] can be simplified further into the expression

$$\chi_M = \frac{N\beta^2}{3kT} [n (n + 2)] \qquad [6]$$

where n is the number of unpaired electrons in the unfilled shell.

b) Multiplet intervals large compared to kT.
This is applicable for most ions of the rare earth elements.

c) Multiplet intervals comparable to kT.
This case involves summation of the contributions of atoms with different values of J. Here departures from Curie's law are observed.

The Weiss Constant[4]

The magnetic susceptibility of many substances may be represented by the Curie-Weiss law $\chi = C/(T + \Delta)$ much better than by the simple Curie law $\chi = C/T$.

Weiss[5] obtained the expression by consideration of the mutual interaction of the elementary magnets on molecular magnetic fields. Δ is referred to as the Weiss constant.

The significance of Δ in the light of the present knowledge is threefold. First Δ appears as an empirical constant from the fact that the multiplet intervals are neither very large nor very small compared to kT. In this case, the Curie

constant C will itself change with temperature, and Δ will have no real significance and will not remain constant over a very large temperature interval. The second source is the inhomogeneous electric fields produced by neighboring ions upon the orbital moment of the electrons. The third source of Δ lies in the Heisenberg exchange interaction. When magnetic atoms or ions are very close together, this interaction has the effect of introducing a very strong coupling between the respective spins. This effect is responsible for the phenomenon of ferromagnetism. The relationship

$$\chi_M = \frac{4\, N\beta S\, (S + 1)}{3\, k\, (T - Tc)} \qquad [7]$$

where

$$T_c = \frac{2\, Jz\, S\, (S + 1)}{3k} \qquad [8]$$

is equivalent to

$$\chi = \frac{C}{(T + \Delta)}$$

Here J is the exchange integral, z is the number of equidistant neighbours with which the atom has exchange coupling. We will see later that this exchange interaction can lead to the phenomena of ferromagnetism and anti-ferromagnetism.

Δ may be obtained experimentally from the intercept of a plot of $1/\chi_M$ against absolute temperature.

Anti-ferromagnetism

The theory of paramagnetic susceptibility discussed earlier applies only to atoms and ions which are free from mutual interaction, i.e. to those which are magnetically dilute. In magnetically concentrated substances, ferromagnetism arises from parallel locking of spin moments between adjacent magnetic atoms or ions, and anti-ferromagnetism arises from an anti-parallel locking of spin moments.

The susceptibility of a typical anti-ferromagnetic substance as a function of temperature has a critical point known as the Néel point. Above the Néel point, most anti-ferromagnetics follow the Curie-Weiss law, below this point, the susceptibility drops and sometimes becomes more or less dependent on the field strength.

Suggestions for understanding the anti-ferromagnetic phenomenon were first made by Néel.[6] It was later developed by Néel,[7] Kramers,[8] Huthén,[9] Bitter,[10] Van Vleck,[11] and others.

Early developments in the theory of anti-ferromagnetism, considering nearest neighbours only suggested equation [8]

$$\Delta = T_c = 2 Jz S (S + 1)/3k \qquad [8]$$

where

J = the exchange integral

z = number of nearest paramagnetic neighbours

S = spin quantum number

k = Boltzmann constant

T_c = temperature at which susceptibility is maximum

More recent developments by Van Vleck[12] are due to the suggestion by Néel that anti-ferromagnetic substances may be regarded as consisting of two sublattices in one of which the atomic moments all orient themselves in one direction while in the other they all orient in the opposite direction. The influence of the second nearest neighbours on a given atom causes Δ to be larger than T_c.

Exchange Mechanisms

Three mechanisms, known as direct exchange, double exchange, and superexchange, may be used to explain the interaction between electron spins. These are based on the Pauli principle.

1. Direct exchange tends to align the net spin on neighbouring lattice elements anti parallel to each other.

2. Double exchange proposed by Zener,[13] requires the transfer of electrons between two kinds of ions, particularly two of the same element but with different charges, and hence is inhibited if these cations are ordered. Double exchange tends to align spins parallel to each other.

3. Kramers[8] suggested the third mechanism, called superexchange which is an indirect mechanism. It is due to an admixture of excited states with the ground state of a system containing two like cations separated by an anion. The excited states are the result of removing an electron from the anion

(say O^{2-}) and placing it in an empty or half filled cation orbital. Indirect magnetic interactions between cations on opposite sides of an anion are:

1) Anti-ferromagnetic if the anion p orbital predominantly overlaps on each side either an empty or half filled cation orbital (case (a) and (c) in fig. 1).

2) Ferromagnetic if the cation orbital is half filled on one side and completely empty on the other (case b).

Goodenough[14] suggested a different mechanism for the indirect magnetic interaction. The mechanism is called "semi-covalent exchange". One of the two electrons in the anion p orbitals participates in semicovalent bonding between the anion and the cation. This electron has a spin parallel to that of the cation since the anion p orbital overlaps an empty cation hybrid orbital. The other electron may participate in semicovalence with a cation on the other side of the anion. This will provide a mechanism for anti-ferromagnetic interaction. This can best be illustrated by fig. 1 case (a).

Crystal field theory[15] was first developed by Bethe,[16] Penney and Schlapp.[17]

In this theory, a transition metal ion in a compound or complex is subjected to an electrostatic field produced by the ligands in its environment. The ligands here are treated as negative ions or as dipolar molecules; in the latter case,

Figure 1. Schematic diagram for three different types of indirect interaction.

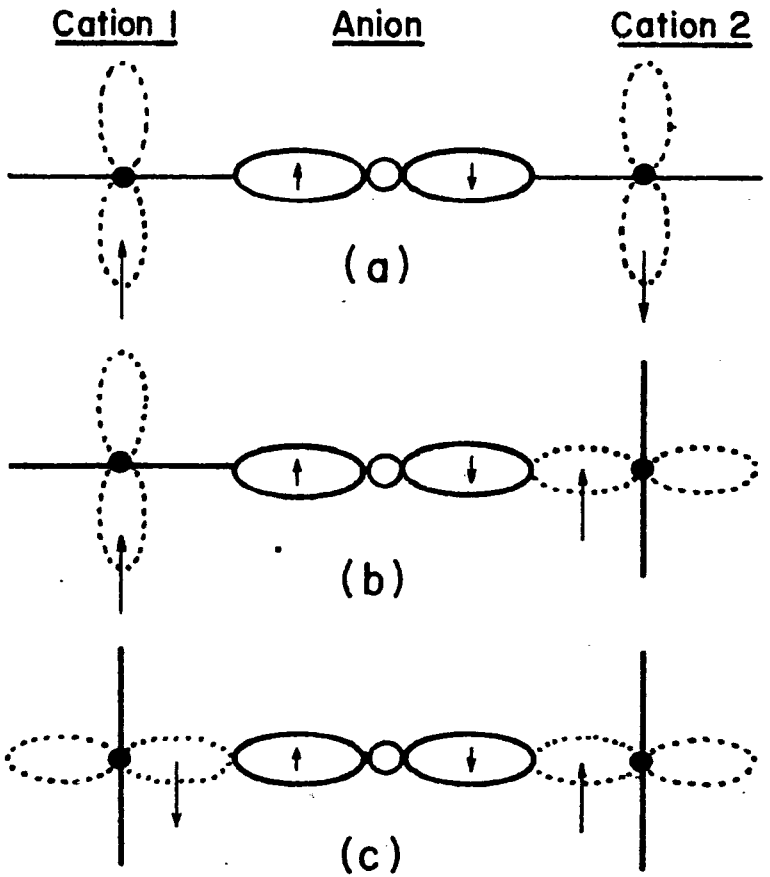
Cation 1
Anion
Cation 2
(a)
(b)
(c)

the negative end of the dipole is invariably directed towards the metal. The effect of the electric field due to the ligands upon the orbital energies of the electrons of the central ion is similar to a Stark effect. In the absence of the field, the five d orbitals and the seven f orbitals are both degenerate, but in the presence of a ligand field of non-spherical symmetry their individual energies are affected differently.

Consider a central ion in an octahedral coordination MX_6. The coordinate axes of the five d orbitals of M lie along MX bond directions. The d_{z^2} and $d_{x^2-y^2}$ wave functions have substantial amplitudes in the direction of the ligands but those associated with orbitals d_{xy}, d_{yz} and d_{xz} do not. A perturbation calculation shows that in a regular octahedral environment the set of five d orbitals splits into two groups. One group is comprised of the three orbitals d_{xy}, d_{yz}, d_{xz} and because of the symmetry properties, this is referred to as the t_{2g} group. The other group consists of the $d_{x^2-y^2}$ and d_{z^2} orbitals and is referred to as the e_g group. In this instance the e_g orbitals have an energy which is higher than that of the t_{2g} orbitals. If the octahedral coordination is not regular, but distorted into a rhombohedral or a tetragonal symmetry, the degeneracy of the d orbitals is reduced even further. The various splittings of the orbital energies are shown in fig. 2.

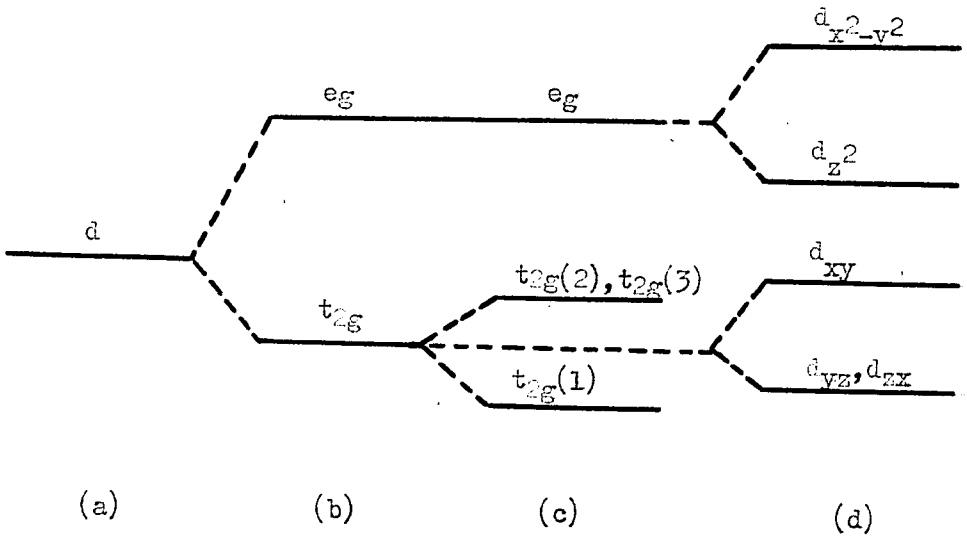

Figure 2. Orbital splittings in fields of various symmetries (a) free atom, (b) cubic, (c) rhombohedral ($\alpha < 60^{\circ}$), (d) tetragonal ($c/a > 1$).

If the energy of the e_g orbitals is E_e and that of t_{2g} is E_t, then the difference $E_e - E_t$ equals 10 Dq and is called the energy separation. The quantity Dq is an empirical parameter of fundamental importance which may be estimated from the optical spectra or in some cases from lattice energies.

In a molecule there are definite electronic levels corresponding to those in the isolated atom, and the orbital groups are filled up gradually according to the "Aufbau" principle starting from the levels of lowest energy. In the distribution of the d electrons between the t_{2g} and e_g orbitals, there is a

competition between the exchange forces which tend to favour the maximum multiplicity (Hund's rule) and the ligand field which tends to force the electrons to occupy, as far as possible, the orbitals of lowest energy. The former is favourable if 10 Dq is small, and this will lead to the "spin free" or "high spin" states. The latter will be realized if 10 Dq is large, and "spin paired" or "low spin" states will be more stable.

The value of 10 Dq depends primarily upon the nature of the ligands and the charge on the central ion. An illustration may be presented for the first transition series.[18,19] (1) For the bivalent ions in the halides 10 Dq falls in the range 7500-12,500 cm^{-1} and for trivalent ions it is in the range 13,500-21,000 cm^{-1}. (2) The common ligands may be arranged so that 10 Dq for their complexes with any given metal increases along the sequence: $I^- < Br^- < Cl^- < F^- < H_2O < CN^-$. (3) Finally 10 Dq for compounds of the second and third series is 40-80% larger than for the corresponding compounds of the first series.

Molecular Orbital Theory of the Bonding in Inorganic Complexes. Ligand Field Theory.

Molecular orbital theory was discussed at an early date by Van Vleck.[20] This theory considers the nature of the bonding between the metal and the ligands. There are both

theoretical and empirical[21] grounds for believing that a considerable amount of coordinate bonding occurs in transition metal complexes. This means that charge transfer from one directed hybrid orbital on each ligand to the metal ion must be allowed for.

In a regular octahedral complex MX_6, the ligand orbitals may combine to form symmetry orbitals and these interact with the metal orbitals. Each interaction between a symmetry orbital of the ligands and an atomic orbital of the metal gives rise to a bonding orbital more stable than either, concentrated mainly on the ligands, and an antibonding orbital less stable than either and concentrated mainly on the metal. The metal orbitals with no counterparts on the ligands contribute nothing to the bonding in a first approximation. This is illustrated in fig. 3.

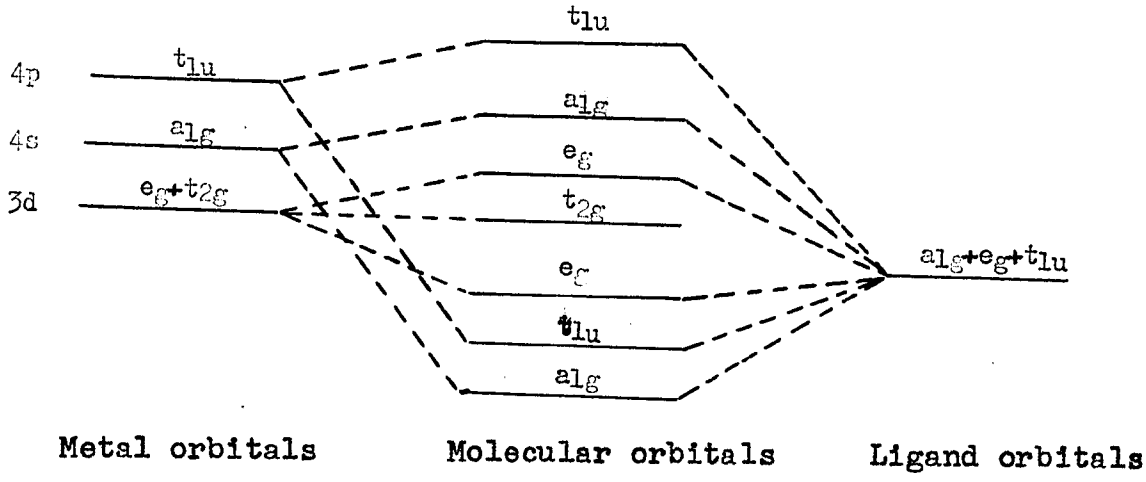

Figure 3. Correlation between atomic and molecular orbitals in octahedral complexes.

In molecular orbital theory in contrast to the crystal field theory some electrons have a certain probability of being on the ligand atoms.

The term "Ligand Field Theory" has been suggested to cover a more general approach to the chemistry of the transition metals. The crystal field theory is adequate provided the electronic wave functions are more or less localized on the central ion, the ligands behaving merely as the source of an electrostatic perturbing potential. When, however, there is strong interaction between the central ion and the ligand orbitals, the transition involves orbitals having a large degree of delocalization over the ligands and the central ion, it is no longer adequate to consider the simple crystal field approximation and instead the ligand field approximation is used, being a combined approach of the molecular orbital theory and the crystal field theory.

B. <u>The Background and the Development of the Problem</u>

In the development of the structural chemistry of transition metal compounds, fluorides have occupied an important position: since the difference in magnetic properties between the strongly paramagnetic complex ions, such as $[FeF_6]^{3-}$, and the weakly paramagnetic complex ions, such as $[Fe(CN)_6]^{3-}$, is the key point in the division of bonds in ferric complexes into two types.

For octahedral complexes the essential distinction is between the use of $3d^2\ 4s\ 4p^3$ hybrid orbitals ("covalent" bonds in Pauling's terminology) and $4s\ 4p^3\ 4d^2$ hybrid orbitals ("ionic").

It is well known that, in the first transition series, the more electronegative ligands such as F, Cl, O favour the use of the higher orbitals, giving compounds with maximum magnetic moments. The fluorides of transition metals are especially interesting, since fluorine is particularly effective in producing abnormally high oxidation states.

Nyholm and Sharpe[22] have made a survey of the available data for transition metal fluorides and fluoro-complexes. Only the results for the first transition series will be tabulated here with a few additional data (table II).

We assume to a first approximation that the magnetic moment should depart from the "spin only" value only because of some orbital contribution or because of indirect exchange coupling governed by principles outlined in figure 1 cases (a) and (c). If this is so, some compounds in table II deserve attention. First of all VF_3, ... has a rather complicated structure but with an octahedral coordination. The vanadium (III) ion is a d^2 (t_{2g}^2) case. The moment of VF_3 is noticeably lower than calculated for the "spin only" value of 2 unpaired electrons. Both spin orbit coupling and indirect exchange in this case will

Table II

Magnetic Moments at 20-24° C

K_2TiF_6	VF_3	CrF_3	MnF_2	FeF_2	CoF_2	NiF_2	CuF_2
0.0	2.55	3.9	5.73	5.59	4.60	2.85	1.57
K_2TiF_6,H_2O	K_3VF_6	K_2CrF_5,H_2O	MnF_3	FeF_3	CoF_3	K_2NiF_4	$CuF_2,2H_2O$
0.0	2.79	3.79	4.94 4.91	-	2.46 2.1	2.97	1.94
	$(NH_4)_3VF_6$	$KCrOF_4$	K_2MnF_5,H_2O	Li_3FeF_6	Li_3CoF_6	K_3NiF_6	K_3CuF_6
	2.79	1.76	3.32	5.87	5.1	2.54	2.8
	K_2VF_5,H_2O		K_2MnF_6	Na_3FeF_6	Na_3CoF_6	$KNiF_3$	$KCuF_3$
	2.74		3.86	5.95	5.3	2.07	1.46
	$(NH_4)VF_4,2H_2O$		$KMnF_3$	$(NH_4)_3FeF_6$	K_3CoF_6	K_2NiF_6	
	2.77		4.89	5.88 5.80	5.15	0.0	
	$VF_3,3H_2O$			K_2FeF_5	Rb_3CoF_6		
	2.79			4.87	5.3		
				$(NH_4)_2FeF_5,H_2O$	Cs_3CoF_6		
				5.91	5.3		
				$FeF_3,3H_2O$	Cs_2CoF_6		
				4.25	2.97		
				$CsFeF_4$	$KCoF_3$		
				4.79	4.03		

Table II (continued)

$KFeF_3$	$Co(NH_3)_6F_3$
4.17	0.0
K_3FeF_6	$Co(NH_3)_3F_3$
6.0	0.0

depress the "spin only" value of the moment, but in the absence of data for various temperatures, calculation of Δ and application of the Curie-Weiss law is not possible.

Nyholm tabulated the magnetic moment of CrF_3 as 3.9 B.M which is in good agreement with the value calculated for 3 unpaired electrons. Without any further explanation this is unexpected since indirect exchange is possible and hence a lower magnetic moment is expected. CrF_3 has a structure in which each chromium atom is surrounded by six fluorine atoms at corners of an octahedron. These octahedra are joined at the corners in three dimensions. The Cr (III) in this case has three unpaired electrons in the t_{2g} group. Spin-orbit coupling should be small but indirect exchange between neighbouring chromium ions through the intervening fluoride ion is expected to occur. The magnetic moment of CrF_3 in Table II was calculated from magnetic susceptibility results obtained by Bizette and Tsai.[23] They found that the susceptibility of CrF_3 follows the Curie-Weiss law between + 20° and -183° C, with a Curie constant of 1.88 and a Weiss constant of + 133° K. Between -183° and -210° C the susceptibility increases with fall of temperature and decreases with increasing field. At -210° C CrF_3 seems to become ferromagnetic.

The moment of MnF_3 is unexpectedly in reasonable agreement with that calculated for four unpaired electrons. Here

the Mn (III) is in octahedral coordination, and is in a spin free state d^4 (t_{2g}^3 e_g). Orbital contribution should be small. The MnF_6 octahedra are joined in three dimensions by sharing corners.[24] It is to be expected that indirect exchange interaction would occur here. In a related case, K_2MnF_5, H_2O, Nyholm observed a reduction of moment which he did not expect, and this compound is being further investigated.

Martin et al[25] on the magnetic susceptibility measurements on compounds with perovskite type structure KMF_3 (where M = Mn, Fe, Co, Ni, Cu) concluded that the low value of the magnetic moments are due to antiferromagnetic interaction.

Ferric fluoride was also studied by Bizette.[23] It shows field dependence at both +20° and -183°C, hence moments are meaningless.

The moments of several complex fluoroferrates have been measured at 20° C. Some slight indication of field strength dependence was obtained for the more concentrated compounds. The "spin only" value is observed for the hexafluoroferrates. It may be doubted whether there can be indirect exchange in the hexafluoro salts, since the p-orbitals of the ligands on neighbouring groups would overlap little if at all and moreover, fluorine cannot engage in $d_\pi - d_\pi$ bonding. In fact, most salts containing discrete hexafluoro anions, e.g. RuF_6^{2-}, MnF_6^{2-}, FeF_6^{3-} appear to be free from indirect exchange effects.[26,27,28]

Hoppe[29] measured the magnetic moments of some alkali fluorometallates and his results are tabulated in Table III.

Table III

Compound	Temp. °K	$\mu_{eff.}$ B.M.	$\mu_{calc.}$ B.M. normal complex	$\mu_{calc.}$ B.M. penetration complex
Li_3CoF_6		5.1	4.90	0
Na_3CoF_6		5.3	4.90	0
K_3CoF_6		5.15	4.90	0
Rb_3CoF_6		5.3	4.90	0
K_3CoF_6		5.3	4.90	0
	90	2.12		
K_3NiF_6	195	2.26	3.87	1.73
	294	2.54		
	90	2.46		
Cs_2CoF_6	195	2.80	5.92	1.73
	294	2.97		

With the exception of the lithium salt, the above M_3CoF_6 compounds and K_3NiF_6 have the same K_3FeF_6 type structure. The M_3CoF_6 compounds are normal complexes (with outer orbitals).

However, K_3NiF_6 did not follow either the Curie or Curie-Weiss law. Hoppe suggested that K_3NiF_6 may be a case of a compound having a paramagnetic central atom which is in a state intermediate between a normal and that of a penetration complex. No proof of this was provided.

Also there seems to be complication in the case of Cs_2CoF_6 and there is no clear explanation of this either as yet. In both cases, indirect exchange is not expected and it was hoped that isomorphous dilution would confirm or deny the view that these compounds are in an intermediate spin state, since if indirect exchange interaction is present, isomorphous dilution should increase the moment. Consequently, such an experiment was strongly indicated. Since it is easier to prepare solid solutions of K_3NiF_6 with an isomorphous diamagnetic host than it would be to prepare solid solutions of Cs_2CoF_6 the former compound was chosen for investigation.

Henkel and Klemm[30] measured the magnetic susceptibility of CoF_2, NiF_2, CuF_2 and CoF_3 and their results are summarized in Table IV.

Table IV

Compound	No. of unpaired electrons	Temp. °K	$\chi_M \times 10^6$	μ_{eff} obs (B.M.)	$\mu_{calc.}$ (B.M.)
CuF_2	1	90	1420	1.01	1.73
		195	1240	1.40	
		293	1050	1.57	
NiF_2	2	90	6240	2.13	2.83
		195	4390	2.62	
		293	3440	2.85	
CoF_2	3	90	22000	4.00	3.88
		195	12100	4.36	
		293	8980	4.60	
CoF_3		90	3510	1.60	
		195	2540	2.00	
		293	2570	2.46	

$\mu_{calc.}$ was obtained from the "spin only" formula. Cobalt in its difluoride is in a "spin free" state d^7 (t_{2g}^5 e_g^2). A considerable orbital contribution is expected in this case. The Ni(II) and Cu(II) ions in the difluorides are likewise in "spin free" states

d^8 ($t_{2g}^6 e_g^2$) and d^9 ($t_{2g}^6 e_g^3$) respectively. In both cases the orbital contribution to the moment should be small. Plots of the values of $\frac{1}{\chi_M}$ against temperature indicate that the Curie-Weiss law is followed approximately for cobalt and nickel difluorides and Weiss constants of $+50^\circ$ K and $+160^\circ$ K were obtained for the cobalt and nickel cases, respectively.

In the cupric difluoride case, it was not possible to obtain the Weiss constant, since it does not follow the Curie-Weiss law or if the best straight line is drawn (plot of $1/\chi_M$ vs T) the Weiss constant obtained is too large to be of any significance. The Jahn-Teller distortion is a further complication here. All of the iron group difluorides have the rutile type structure which is distorted in the cases CrF_2 and CuF_2.

A positive Weiss constant has a real significance and can be used to evaluate the moment according to the expression $\mu = 2.83 \sqrt{\chi_M \times (T + \Delta)}$ only when it is established that the deviation from Curie's law is caused by anti-ferromagnetic interaction. This is especially important when the Weiss constant obtained is large as in the case of NiF_2. The technique of isomorphous dilution is sometimes employed to confirm the presence or absence of anti-ferromagnetic interaction in a substance.

The value for CoF_3 has been confirmed by Nyholm and Sharpe.[22] For this compound there is also a temperature

dependence at least up to 293° K, but the Curie-Weiss law is not obeyed; hence the limiting value of μ is certainly greater than 2.5 B.M. CoF_3 has a structure in which each cobalt atom has six octahedrally arranged fluorine atoms as nearest neighbours. Tervalent cobalt is d^6; if the bonds were $3\,d^2\,4s\,4p^3$ the compound would be diamagnetic, but the use of "ionic" or $4s\,4p^3\,4d^2$ bonds requires a moment of 4.90 B.M. Nyholm suggested that with the exception of the M_3CoF_6 series, in which moments indicate 4 unpaired electrons, tervalent cobalt in its complex compounds resembles the second and third transition series much more than those of the first.

Westland and Hoppe,[31] after several attempts obtained a sample of K_2NiF_4 which obeyed the Curie-Weiss law with a Weiss constant of +140° K. The magnetic susceptibility of that sample is given in Table V.

Table V

Temp. °K	$\chi_g \times 10^6$	$\chi_M \times 10^6$	μ_{eff} B.M.	μ (B.M.)
90	17.60	3830	1.66	2.66
195	12.00	2640	2.03	2.66
292	9.20	2040	2.18	2.65

Other attempts have resulted in magnetic susceptibilities characteristic of an anti-ferromagnetic substance below the Néel

point, e.g. the susceptibility decreased with decreasing temperature. K_2NiF_4 has a structure which is ideally suited for indirect exchange interaction. Isomorphous dilution would decrease this interaction and hence should increase the effective moment.

The behaviour described above is, for the most part, roughly in agreement with simple magnetic theory modified by the inclusion of the indirect exchange mechanisms "a" and "c" on page 12. The triflorides VF_3 and MnF_3 appear anomalous however. Further more, the precise behaviour of certain substances, e.g. the slight departure from the Curie-Weiss law in the case of NiF_2, is not accounted for by simple theory. Consequently, it appeared desirable to reinvestigate VF_3 and MnF_3 and to subject some typical fluorides, those of nickel, to a more detailed study by means of isomorphous dilution in a diamagnetic "host" compound.

EXPERIMENTAL

A. Magnetic Susceptibility Measurements

The Gouy method was used for the susceptibility measurements. In this method the specimen takes the form of a rod of uniform cross section, one end of which is situated in a region of large field strength H and the other in a region of small field H_o. Integration over the range of field gradients involved, leads to the expression for the force which acts on the rod.

$$F = \frac{1}{2} A \chi (H^2 - H_o^2) \qquad [9]$$

where A = cross sectional area.

χ = volume susceptibility.

In practice, H is the field at the centre of the pole gap between the magnets, and H_o is very small or zero, being the field in a region out of the influence of the magnet.

Equation [9] holds if the atmosphere surrounding the sample has negligible susceptibility. If the sample is suspended in air, the expression becomes

$$F = \frac{1}{2} A (H^2 - H_o^2) (\chi - \chi') \qquad [10]$$

where χ' is the susceptibility of air, which is equal to $+ 0.029 \times 10^{-6}$ c.g.s units/cc at 20° C.

In practice the sample tube was evacuated and if the condition of zero field at the outer end of the tube can be achieved (sufficiently long sample), then equation [10] can be simplified to

$$F = \frac{1}{2} A \kappa H^2 \qquad [11]$$

The technique employed was to measure the difference in force developed on the application and removal of the field H. The apparatus used is shown diagramatically in fig. 4.

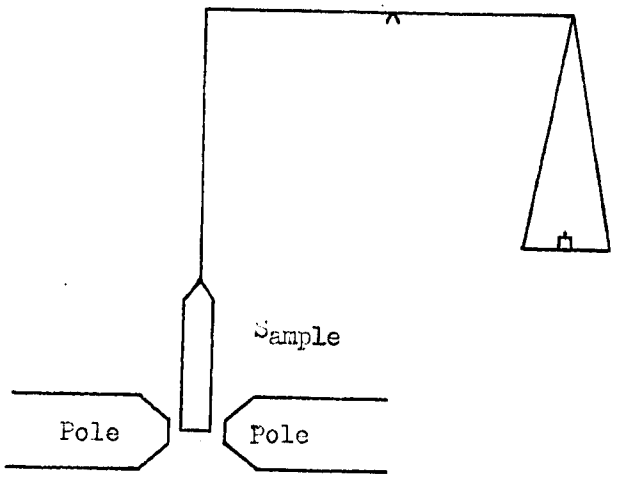

Fig. 4. Apparatus for the Gouy method.

If the apparent change of weight of the sample upon the application of the magnetic field H is ΔW then

$$F = g\Delta W = \frac{1}{2} A \kappa H^2 \qquad [12]$$

where g is the gravitational constant, and further

$$\kappa = \frac{2g \Delta W}{A H^2}$$

and to obtain gram susceptibility we have

$$\chi_g = \frac{2 g l \Delta W}{H^2 m} \qquad [13]$$

where l and m are the length and the mass of the sample, respectively.

The Samples

The samples were all in powder form and were contained in a pyrex tube. The dimensions of the tube were: outer diameter = 3 mm., inner diameter = 1.5 mm. and the length of the tube = 8.60 cm.

In order to obtain reasonable accuracy in the measurement of the susceptibilities, it is essential to pack the sample uniformly. This was done by sealing the tube to another tube with larger diameter and having a ground glass joint at the other end. Small quantities of the powder were introduced into the tube and the bottom of the tube was then tapped firmly on a wooden surface. This process was continued until the tube was filled up to the necessary length, usually 6-8 cm. Then

the tube was evacuated and was sealed off at the upper end. A hook was made at this end and the tube was suspended by means of a quartz fibre from the left hand pan of the magnetic balance. At this stage care was taken to ensure that (i) the tube with content was vertically placed (ii) the bottom end of the sample was in the middle between the pole pieces horizontally (iii) the magnet was aligned so that the tube and content was placed centrally between the pole pieces.

The tube, quartz fibre and turnbuckle were enclosed in a glass jacket, so that they were protected from air currents. The glass jacket was covered all along with asbestos string.

Correction for the Empty Tube

The tube itself comprises a form of hollow specimen and consequently develops a force which is always present and which has to be subtracted from the observed force in order to obtain the force on the sample alone. The force is usually negative since the glass is diamagnetic. The correction for the empty glass was obtained by measuring the apparent change of weight of the evacuated tube alone, when the magnetic field was applied.

The corrections for the tube used in subsequent measurements are given in Table VI.

Table VI

Current	Temperature 295-302° K	224.5° K	195° K	90° K
2.5 Amp.	-.047 mg.	-.050 mg.	-.050 mg.	-.056 mg.
5.0 Amp.	-.200 mg.	-.209 mg.	-.209 mg.	-.226 mg.
7.5 Amp.	-.435 mg.	-.435 mg.	-.435 mg.	-.494 mg.
10.0 Amp.	-.649 mg.	-.648 mg.	-.648 mg.	-.745 mg.

The Description of the Balance

An Ainsworth projection type micro balance was used for measuring the apparent change of weight when magnetic field was applied. Weighings were carried out under the same conditions every time by the method of swings. The sensitivity of the balance was determined before measurements at each temperature.

In order to obtain the correct value for the change in weight when field was applied, it was of particular importance, especially for low temperature measurements, that rest points were recorded before and after every reading to obtain the mean.

The Magnet

An electromagnet was used. It possessed truncated pole pieces, with a gap between them of 1.9 cm. The electromagnet is adjustable in two horizontal directions at right

angles to each other.

Measurements were made at four different field strengths obtained by using currents of 2.5; 5.0; 7.5; and 10.0 amps.

The current was drawn from a set of lead accumulators, adjusted by two rheostats, and was measured by a Bach-Simpson Ltd., Model 9 Ammeter with an accuracy of ± 0.5%.

Calibration of the Field Strength

Although it is possible to use the Gouy method directly for absolute measurements of magnetic susceptibility by measuring H, A, etc., this is rarely done. Instead, the apparatus is calibrated by means of a substance of known susceptibility. In the present work, hydrated ferrous ammonium sulphate (Mohr's salt) was used. The gram susceptibility is given by Selwood[4] as

$$\chi_g = 9500 \times 10^{-6}/(T + 1) \qquad [14]$$

where T is the absolute temperature.

Chemically pure Mohr's salt was recrystallized from water, dried, and finely powdered before packing uniformly in the tube.

The measurements were done at room temperature and the value of H^2 was calculated from equation [14]. The average value of three measurements are given in Table VII.

Table VII

Currents in Amps.	Field Strength in Oersteds
2.5	1454
5.0	2937
7.5	4354
10.0	5349

Magnetic Measurements of Different Samples

The measurements were carried out at different temperatures: room temperature, 224.5° K, 195° K and 90° K. The temperatures were measured with a copper-constantan thermocouple. For low temperature work, the lower end of the glass jacket was immersed in a coolant contained in a specially constructed Dewar flask which fitted between the pole pieces.

The gram susceptibility was calculated using expression [13] after the necessary correction for the empty tube.

Usually the samples showed a slight ferromagnetism so it was necessary to obtain the value of χ_g at infinite field by extrapolating the plot of χ_g against 1/H.

The gram susceptibilities of the paramagnetic ion in the solid solutions were calculated by using Wiedemann's

additivity law

$$\chi = \chi_1 m_1 + \chi_2 m_2 \qquad [15]$$

where χ is the experimentally determined susceptibility and χ_1, χ_2, m_1 and m_2 are the susceptibilities and weight fractions of the two components, respectively. The molar susceptibility of the paramagnetic compound is obtained from

$$\chi_M = \chi_g \times M - \sum \chi_A \qquad [16]$$

where M is the molecular weight of the paramagnetic compound, χ_g is the gram susceptibility of the paramagnetic compound and χ_A is the diamagnetic susceptibility of each of the paramagnetic atoms.

Magnetic moments were calculated using the equation

$$\mu_{eff} = 2.83 \sqrt{\chi_M \times T} \qquad [17a]$$

or

$$\mu = 2.83 \sqrt{\chi_M \times (T + \Delta)} \qquad [17b]$$

Precision and Accuracy of the Magnetic Measurements

These were determined by Bhiwandker.[32] The largest error was probably due to non-uniformity of packing and it amounted to about ± 2%.

B. Preparation of Samples

Magnesium Difluoride MgF_2

This can be prepared in a wet way by the precipitation from a solution of magnesium sulfate by potassium fluoride. In the present work, MgF_2 was prepared by the fluorination of reagent grade anhydrous magnesium sulfate, $MgSO_4$, since this method seemed to be favourable for the preparation of the solid solutions of MgF_2 and NiF_2.

A known weight of finely powdered $MgSO_4$ was placed in a small porcelain boat, and was fluorinated at a temperature of 250° C for 2 hours. The furnace was allowed to cool to room temperature without interrupting the fluorine stream before removing the product this was again weighed to ensure the completeness of the reaction.

Nickel Difluoride NiF_2

Nickel difluoride was prepared by fluorinating nickel sulfate monohydrate $NiSO_4 . H_2O$.

Reagent grade $NiSO_4.6H_2O$ was heated in an oven at 120-130° C for at least 12 hours to obtain the monohydrate $NiSO_4.H_2O$. This was then finely powdered and was fluorinated at 250° C for 2 hours. After the product was sufficiently cool, the fluoride was transferred to a vacuum system using a suitable transferring device. The sample was then heated in vacuum for

2 hours at 400° C to bring the nickel of the higher oxidation states to the bivalent state. The product was pure yellow. Analysis: Ni calculated = 60.7%, found = 59.5%.

The Mixed Sulfates (Ni, Mg) $SO_4.6H_2O$

Various proportions of reagent grade $NiSO_4.6H_2O$ and $MgSO_4$ were dissolved in water to obtain a saturated solution. The solution was heated almost to boiling and filtered. The filtrate was evaporated slowly and precipitated rapidly using an ice-salt bath as a coolant. The fine crystals were filtered off and dried under suction.

The Solid Solutions of Nickel Difluoride and Magnesium Difluoride

These were prepared by the fluorination of the corresponding mixed sulfates.

Samples of (Ni, Mg) $SO_4.6H_2O$ of various compositions were heated in an oven at 120-130° C to obtain the monohydrate. They were then finely powdered and fluorinated at 250° C for 2 hours and subsequently heated in a vacuum for 2 hours at 400° C. The products were various shades of light yellow.

X-ray diffraction patterns were obtained to ensure the homogeneity of the solid solutions.

Potassium Magnesium Sulfate $K_2Mg(SO_4)_2.6H_2O$

This was prepared using the solubility data of Klooster.[33]

In the present preparation, a 60:40 weight proportion of $MgSO_4$ to K_2SO_4 was dissolved in water to obtain a saturated solution. The solution was heated almost to boiling and filtered. The filtrate after being concentrated slowly, was allowed to crystallize at room temperature. The crystals were dried out under suction before storing them in a desiccator.

Potassium Nickel Sulfate $K_2Ni(SO_4)_2.6H_2O$

This was prepared using the solubility data of Caven and Johnston.[34] A 50:50 weight proportion of $NiSO_4$ to K_2SO_4 was used in this preparation to obtain $K_2Ni(SO_4)_2.6H_2O$. After similar treatment as in the case of $K_2Mg(SO_4)_2.6H_2O$, green crystals of $K_2Ni(SO_4)_2.6H_2O$ were obtained.

The Mixed System $K_2(Ni, Mg)(SO_4)_2.6H_2O$

Taking into consideration the phase diagrams for the preparation of both $K_2Mg(SO_4)_2.6H_2O$ and $K_2Ni(SO_4)_2.6H_2O$, a mixture of reagent grade K_2SO_4, $MgSO_4$ and $NiSO_4.6H_2O$ in certain proportions were dissolved in water to obtain a saturated solution. After similar treatment as before, the saturated filtrate was cooled rapidly using an ice-salt bath. The resulting fine crystals were separated by filtration and dried.

Potassium Cyanonickelate $K_2Ni(CN)_4$

This was prepared by dissolving an excess of nickel

cyanide $Ni(CN)_2$ in potassium cyanide solution until it was saturated. The excess nickel cyanide was filtered off and the hydrated $K_2Ni(CN)_4$ was crystallized from the filtrate. The crystals were then heated in an oven at 120-130° C to obtain the anhydrous $K_2Ni(CN)_4$.

Potassium Magnesium Fluoride K_2MgF_4

This was prepared by the fluorination of the corresponding sulfate.

$K_2Mg(SO_4)_2.6H_2O$ was first heated in an oven at 120-130° C to form the monohydrate. The crystals were powdered finely and fluorinated at 300° C for 2 hours. The product was heated in vacuum at 450-475° C for 2 hours to provide a similar treatment as was given the nickel analogue.

Analysis: Mg calculated = 13.62%, found = 13.92%.

Potassium Nickel Fluoride K_2NiF_4

This was prepared in the same manner as in the case of K_2MgF_4, using $K_2Ni(SO_4)_2.6H_2O$ as the starting material, and this was first converted to the monohydrate before the fluorination.

The product of fluorination was fuschia in colour (K_2NiF_6). This was heated in vacuum at 450-475° C for 4-6 hours to obtain the pale yellow K_2NiF_4.

Applying the same procedure as the above, K_2NiF_4 can also be obtained using $K_2Ni(CN)_4$ as the starting material.

Analysis: Ni calculated = 27.57%, found = 27.40%.

The Solid Solutions of K_2MgF_4 and K_2NiF_4

These were prepared by the fluorination of the corresponding mixed sulfates monohydrate at 300° C for 2 hours. Then it was heated in vacuum at 450-475° C for 4-6 hours.

X-ray diffraction patterns were taken for K_2MgF_4, K_2NiF_4 and their solid solutions.

Potassium Nickel (III) Hexafluoride K_3NiF_6

An equivalent mixture of anhydrous potassium nickel sulfate $K_2Ni(SO_4)_2$ and potassium sulfate were used for this preparation.

First $K_2Ni(SO_4)_2.6H_2O$ was heated in a muffle furnace at 350° C for at least 10 hours to obtain the canary yellow anhydrous $K_2Ni(SO_4)_2$. This was then mixed intimately with K_2SO_4 to give a 2:1 mole proportion of $K_2Ni(SO_4)_2$ to K_2SO_4. This mixture was fluorinated at 450° C for 4 hours. The product was fuschia (mostly K_2NiF_6 + KF_x). But after it was heated in vacuum for 4 hours at 300° C the final product was the lilac coloured K_3NiF_6, which was rather unstable. It was stored in an ampule containing dry nitrogen.

The same procedure can also be applied to a mixture of 1:1 mole proportion of KCl to $K_2Ni(CN)_4$. K_3NiF_6 was also prepared according to Klemm and co-workers[35] In this preparation,

the fluorination of the mixture of the sulfates was carried out at 340° C for 2 hours. But in this case the fluorine gas was diluted with anhydrous CO_2 to give 5:4 volume proportion of F_2 to CO_2. The product obtained was lilac.
Analysis: Ni calculated = 20.24%, found = 19.51%.

Potassium Aluminum Alum $KAl(SO_4)_2.12H_2O$

This was prepared using the solubility data of Britton.[36]

Potassium Cryolite $K_{2.8}AlF_{5.8}$

This was prepared by the fluorination of a mixture of $KAl(SO_4)_2$ and K_2SO_4 in a mole proportion of 1 to 0.9, respectively.

$KAl(SO_4)_2$ was first obtained by heating the alum in a muffle furnace at 325° C for 24 hours. This was mixed intimately with the correct proportion of K_2SO_4 and subsequently fluorinated at 340° C for 2 hours. The fluorine gas was diluted with CO_2 in the same manner as for the preparation of K_3NiF_6. Weights of the sample were recorded before and after the fluorination, and that of the fluorination product agreed with the expected value for $K_{2.8}AlF_{5.8}$

The Solid Solutions of $K_{2.8}AlF_{5.8}$ and K_3NiF_6

A mixture of the sulfates for the preparation of

K_3NiF_6 and that for $K_{2.8}AlF_{5.8}$ was prepared in various proportions. The intimately mixed sample was fluorinated for 2 hours at 340° C. In this case again the fluorine was diluted with CO_2 as before.

The X-ray diffraction patterns of the solid solutions could not have revealed any inhomogeneity in the solid solutions since the X-ray diffraction pattern of $K_{2.8}AlF_{5.8}$ and K_3NiF_6 are very much alike in dimension as well.

Manganese Sesquioxide Mn_2O_3

The procedure of Meyer and Rötgers[37] was used using manganese dioxide MnO_2 as the starting material.

Ammonium Pentafluoromanganate (III) $(NH_4)_2MnF_5$

Manganese sesquioxide Mn_2O_3 was dissolved in concentrated hydrofluoric acid in a platinum dish. The dark purple solution was added to a saturated solution of ammonium fluoride in a teflon beaker. A pinkish fine precipitate was formed and this was recrystallised from water containing ammonium fluoride. The precipitate was first air dried and then dried further under vacuum at room temperature for 24 hours.

Manganese Trifluoride MnF_3

The method employed was based on that of Hoppe.[38]

$(NH_4)_2MnF_5$ was fluorinated for 2 hours, starting at room temperature and gradually raising the temperature to 250° C.

The fluorine gas was diluted with dry nitrogen in order to slow down the reaction.

The purplish MnF_3 was unstable; it changed into a brownish substance fairly quickly in air, and was kept in a glass ampule containing dry nitrogen.

Analysis: Mn calculated = 49.08%, found = 46.74%.

Vanadium Trioxide V_2O_3

The preparation was based on the procedure by Spencer and Justice.[39]

Technical grade V_2O_5 was the starting material, and this was first purified.

Vanadium trioxide was then prepared from the purified pentoxide by heating it in a stream of hydrogen at 475° C for 3 hours.

Vanadium Trifluoride VF_3

The method used here was based on the procedure of Carpenter and co-workers.[40]

Vanadium trioxide was treated with anhydrous HF gas in the fluorination furnace at room temperature for one hour. After this period of time, the temperature was gradually raised to 460° C (maximum temperature possible for the furnace). The HF flow was continued for 4 hours at this temperature and also during the process of cooling. When the furnace had cooled

to 60° C, the sample was purged with dry argon to remove the adhering HF. The green product was pulverized in an anhydrous N_2 atmosphere and was stored in an ampule.

Analysis: V calculated = 47.20%, found = 46.25%.

C. Analyses

Duplicate determinations were carried out in each case. All weighings were done under conditions approaching 50% relative humidity. The balance used was a Sartorius-Werke projected scale semimicro balance.

Determination of Magnesium

In K_2MgF_4. A weighed sample contained in a platinum dish was treated with a small quantity of concentrated H_2SO_4 and was heated on a hot plate to dissolve the sample and to expel the HF formed. The solution was transferred to a beaker and was diluted with distilled water to a total volume of 150 mls.

Magnesium was then determined gravimetrically as the pyrophosphate. Pure diammonium phosphate $(NH_4)_2HPO_4$ was used as the precipitating agent and double precipitations were carried out to obtain a precipitate of the proper composition.

Determination of Nickel

In NiF_2 and the solid solutions $(Ni,Mg)F_2$. The compositions of the pure compound and the solid solutions were established by determining the Ni content gravimetrically with dimethyl-

glyoxime. Samples were decomposed in a manner similar to that used in the case of K_2MgF_4.

Solutions of known Ni content with varying Mg concentrations both as the sulfate, were analysed for preliminary investigation. It was found that a concentration of Mg in the mixture as high as 95 atomic % did not interfere with the Ni analysis.

The results of the analyses of various solid solutions are given in Table VIII.

Table VIII

Composition of solid solutions $(Ni,Mg)F_2$

Product No.	Wt. % Ni	Wt. % NiF_2	Atom % Ni
1	36.58	60.30	49.48
2	20.98	34.56	25.39
3	12.56	20.69	14.39
4	12.25	20.20	14.03
5	5.61	9.25	6.16
6	5.00	8.24	5.48

Ni in K_2NiF_4 and the solid solutions $K_2(Ni,Mg)F_4$. Ni content was determined as described previously. In some cases, the filtrates remaining after the Ni determination were analysed

for their Mg content by the pyrophosphate method in order to verify the composition of the solid solutions.

The results of the analyses are given in Table IX.

Table IX

Composition of solid solutions $K_2(Ni,Mg)F_4$

Product No.	Wt. % Ni	Wt. % K_2NiF_4	Atom % Ni
1	19.56	70.95	67.19
2	16.44	59.63	55.30
3	14.84	53.83	49.50
4	14.20	51.51	47.19
5	12.47	45.23	40.91
6	9.00	32.64	28.89
7	4.75	17.23	14.89
8	1.79	6.49	5.50

Ni in K_3NiF_6. The sample was treated with 10 mls of dilute H_2SO_4 (1:1). Evolution of gas was observed and the sample dissolved quite readily. The solution was evaporated slowly on a hot plate. It was then transferred to a glass beaker and diluted with distilled water to a volume of 150 mls. The Ni content was determined by the usual method.

Ni in the solid solutions of K_3NiF_6 and $K_{2.8}AlF_{5.8}$. Decomposition of the samples was carried out as indicated in the case of K_3NiF_6.

The resulting solution was diluted with water and approximately 3 grams of ammonium chloride and a few drops of methyl red indicator were added. The solution was heated to boiling and dilute ammonium hydroxide (1:2) was added slowly until the colour of the solution changed to a distinct yellow. The solution was boiled for 1-2 minutes and the $Al(OH)_3$ precipitate was separated immediately by filtration through paper. The precipitate was washed thoroughly with hot 2% ammonium chloride solution and the filtrate was analysed for the Ni content as usual.

The results of analysis of the solid solutions are given in Table X.

Table X

Composition of solid solutions of $K_{2.8}ALF_{5.8}$ and K_3NiF_6

Product No.	Wt. % Ni	Wt. % K_3NiF_6	Atom % Ni
1	2.05	10.13	8.75
2	4.89	24.15	21.30

Determination of Manganese

In MnF_3. A weighed sample contained in a platinum dish was treated with few ml. of concentrated H_2SO_4 and was evaporated on a hot plate until dense white fumes were evolved.

The solution was transferred to a beaker using a small quantity of distilled water. At this stage fine brownish particles were still undissolved but after the addition of 2 ml. of 30% H_2O_2 a completely clear and colorless solution was obtained.

The oxidation of Mn (II) by sodium bismuthate was done in a nitric acid solution containing approximately 22% by weight of concentrated HNO_3. Sodium bismuthate was added until some was left undissolved. The residue was separated by filtration through a sintered crucible and it was washed with cool 3% nitric acid solution until free from permanganic acid. Ferrous sulfate was added to reduce Mn(VII) to the bivalent state and excess ferrous ion was titrated with standard permanganate solution.

Determination of Vanadium

In VF_3. The sample was dissolved in concentrated HF. The resulting solution was evaporated on a water bath, 10 ml. of dilute H_2SO_4 (1:1) were added and the solution again evaporated to expel the remaining HF.

The green solution was diluted with freshly boiled

water to a volume of 100 mls. A 0.1 N standard $KMnO_4$ solution was added dropwise until the solution was slightly pink. It was then poured through a Jones reductor and collected in a beaker containing 100 ml. of 10% ferric alum solution [$Fe(NH_4)(SO_4)_2.12H_2O$]. The resulting ferrous ion was titrated with standard 0.1 N $KMnO_4$ solution.

Results and Discussion

The results of the magnetic susceptibility measurements on pure compounds and various solid solutions are given in tables XI, XII, XIII, XIV, XV, XVI

Table XI

Results of magnetic measurements on pure compounds

Compound	Temp. ^{o}K	$\chi_g \times 10^6$	$\chi_M \times 10^6$	μ_{eff} B.M.	μ
VF_3	300	24.40	2731	2.56	
	195	29.80	3326	2.28	
	90	47.80	5309	1.96	
*MnF_3 + silica	297	6.11	10713	5.05	4.94
	195	9.38	16453	5.07	4.91
	90	22.08	38640	5.28	4.91
Silica	298	-0.166			
	195	-0.142			
	90	-0.194			

Table XI, continued

K_2NiF_4	298	8.80	1959	2.16	
	195	8.09	1806	1.68	
	90	6.66	1500	1.04	
K_2MgF_4	297	-0.362			
	90	-0.360			
NiF_2	298	34.60	3444	2.87	3.61
	224.5	41.60	4144	2.73	3.64
	90	60.30	5984	2.08	3.56
K_3NiF_6	301.5	8.60	2689	2.55	
	195	10.00	3112	2.20	
	90	21.00	6422	2.15	
$K_{2.8}AlF_{5.8}$	301	-0.279			
	195	-0.322			
	90	-0.478			

χ_g at a given temperature was calculated for every field strength. There was a slight field dependence. To correct for this, χ_g values for the various temperatures were plotted against $\frac{1}{H}$ and χ_g tabulated was obtained as the extrapolated value at infinite field. The values of χ_M are reported after the correction for the diamagnetism of the various ions including the underlying diamagnetism of the paramagnetic ion itself.

*MnF_3 had to be diluted in the form of a mechanical mixture with silica as the apparent change of weight when the field was applied was too large for accurate measurements when the pure compound was used.

The results will be discussed separately for each paramagnetic ion.

The Configuration $d^2(t_{2g}^2)$ Vanadium (III)

The effective moment of VF_3 shows a temperature dependence. The room temperature value agrees with that obtained by Nyholm and Sharpe,[22] who obtained a value of 2.55 BM at 20° C. The present result shows that μ_{eff} decreases with decreasing temperature and that the Curie-Weiss law is not obeyed as can be seen from Fig. 5.

Vanadium (III) in an octahedral coordination is a t_{2g}^2 case. A moment of 2.83 B.M is to be expected for two unpaired electrons. Spin-orbit coupling might decrease the moment since the shell is less than half filled. Further,

Figure 5. Plot of $1/\chi_M$ vs T for VF_3.

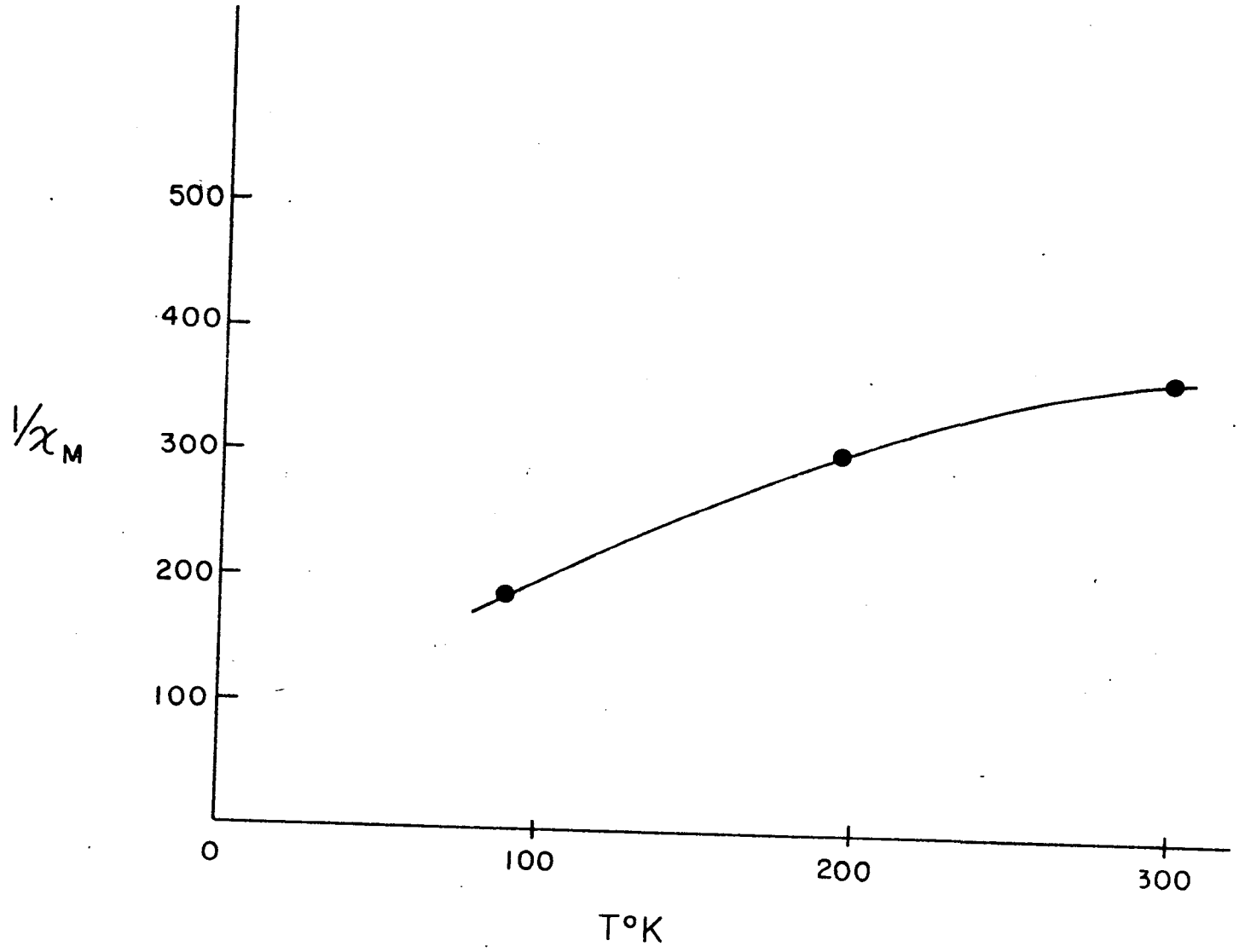
500
400
$1/\chi_M$
300
200
100
0
100
200
300
T°K

indirect exchange might decrease the moment by the mechanism of case (a) in Fig. 1. However E.D. Wollan[41] found no evidence from neutron diffraction studies of superlattice reflection characteristic of anti-ferromagnetic structure in VF_3 even at a temperature as low as 4.2° K.

Figgis[42] has calculated and obtained a graphical representation of the magnetic moment as a function of the parameter $kT/|\lambda|$ for Vanadium (III) ion in an octahedral environment. λ is the spin-orbit coupling constant for the free ion which is equal to 105 cm^{-1} for Vanadium (III) ion. From the plot it can be seen that μ_{eff} decreases with decreasing $kT/|\lambda|$ for both medium and weak ligand fields. Figgis' curves are reproduced in Fig. 6.

The present μ_{eff} values of VF_3 at room temperature and 195° K is in agreement with the medium field approximation, but that of 90° K is considerably higher, the value being closer to the weak-field approximation. The moment of Vanadium trifluoride does not exactly follow the theory and this may be for several reasons. The field strength is possibly intermediate between weak and medium, and the assumption of a free ion in a field of perfect cubic symmetry, upon which the plot was based, is not entirely true in this case. The compound has a rather complicated structure which is shown in Fig. 7. The unit cell is rhombohedral[43] with dimensions: $a = 5.37 \pm 0.002$ A°, $\alpha = 57.52 \pm 0.03^\circ$. The octahedron of F atoms

Figure 6. μ_{eff} vs. $kT/|\lambda|$ for V^{3+} (λ positive).

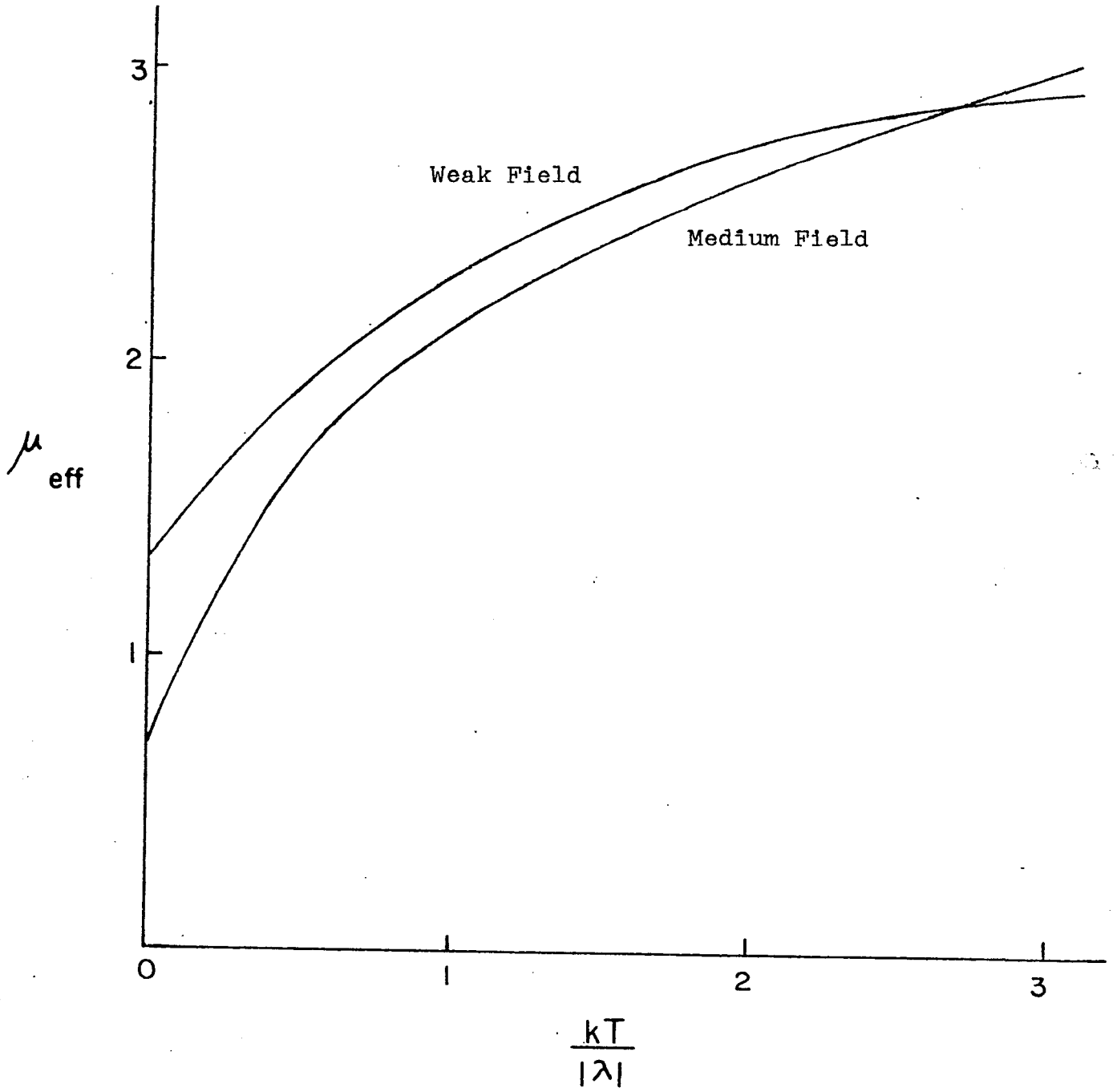
3
2
1
0
1
2
3
Weak Field
Medium Field
μ_{eff}
$\frac{kT}{|\lambda|}$

Figure 7. The structure of VF_3.

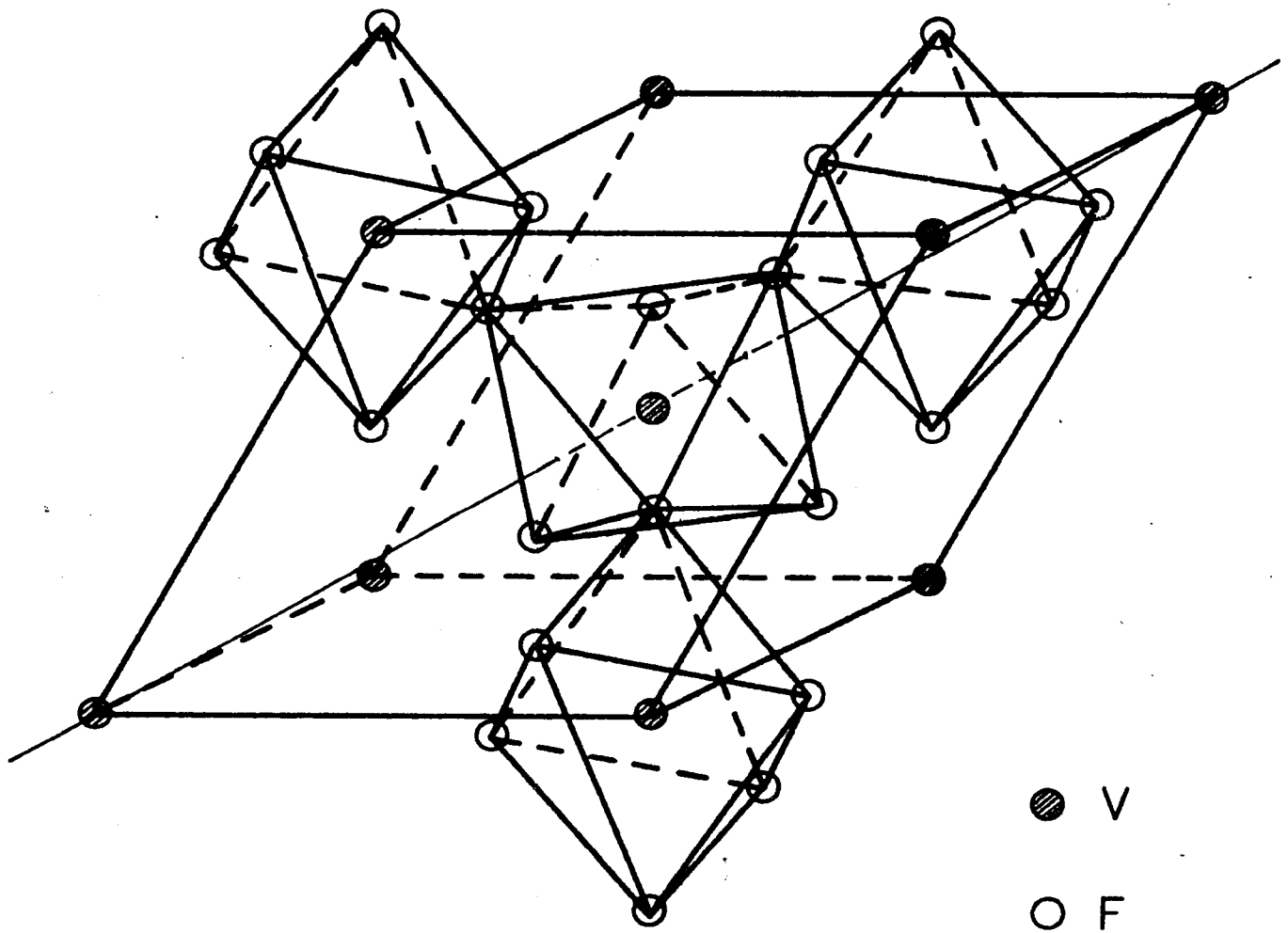
V
F

around each V atom is not regular; there is some distortion of the cubic symmetry.

The temperature dependence of the moment of VF_3 may not entirely be due to spin-orbit coupling, but also to indirect exchange interaction. Although the V-F-V bond angle in VF_3 is not ideal for indirect exchange, nevertheless it is believed that indirect exchange between neighbouring vanadium atoms is not completely eliminated. However, a definite proof to establish this view cannot be gained from susceptibility measurements alone. An experiment which may decide this question of possible indirect exchange is the isomorphous dilution of VF_3. There is a difficulty in such an experiment, however, as there is no diamagnetic trifluoride with a VF_3 type structure that can serve as a host lattice. It may, however, be possible to prepare solid solutions of VF_3 and AlF_3, up to a certain concentration of the former while the system retains the VF_3 structure.

It is consequently not possible at present to draw inferences from the behaviour of VF_3 which could serve to establish a theory of indirect exchange for transition metal fluorides.

The Configuration $d^4(t_{2g}^3 e_g)$ Manganese (III)

The results of magnetic measurements on MnF_3 are given in Table XI.

The Curie-Weiss law is obeyed, at least to temperatures as low as 90° K and a Weiss constant of -12° K was obtained from a plot of $\frac{1}{\chi_M}$ against T in Fig. 8. The moment calculated according to the formula $\mu = 2.83 \sqrt{\chi_M(T - 12)}$ gives an average value of 4.92 B.M, in good agreement with that obtained by Nyholm and co-workers.[24]

Anti-ferromagnetism, which is expected to occur in MnF_3, is generally associated with a positive Weiss constant. During the present investigation the author encountered a paper by Bozorth and Nielsen[44] in which it was reported that anti-ferromagnetism is present in MnF_3, with a Néel point of + 47° K and a Weiss constant of - 8° K. They also came to the conclusion that the Curie-Weiss law is obeyed above 50° K and obtained a moment of 5.0 B.M. E.O. Wollan[41] and co-workers found evidence of anti-ferromagnetism from neutron diffraction studies of MnF_3. The compound shows a growth of superlattice reflections at low temperatures but anti-ferromagnetism in this case is different than in other trifluorides of the iron group (CrF_3, FeF_3, CoF_3). Wollan found the Néel temperature to be + 43° K.

The crystal structure of MnF_3 is monoclinic[24] with dimensions: a = 8.904 ± 0.003 A°, b = 5.037 ± 0.002 A°, c = 13.448 ± 0.005 A°; β = 92.74 ± 0.04°. There are 12 molecules per unit cell, but the basic anti-ferromagnetic structure can most easily be described in terms of an idealized cubic form as in Fig. 9.

Figure 8. Plot of $1/\chi_M$ vs. T for MnF_3.

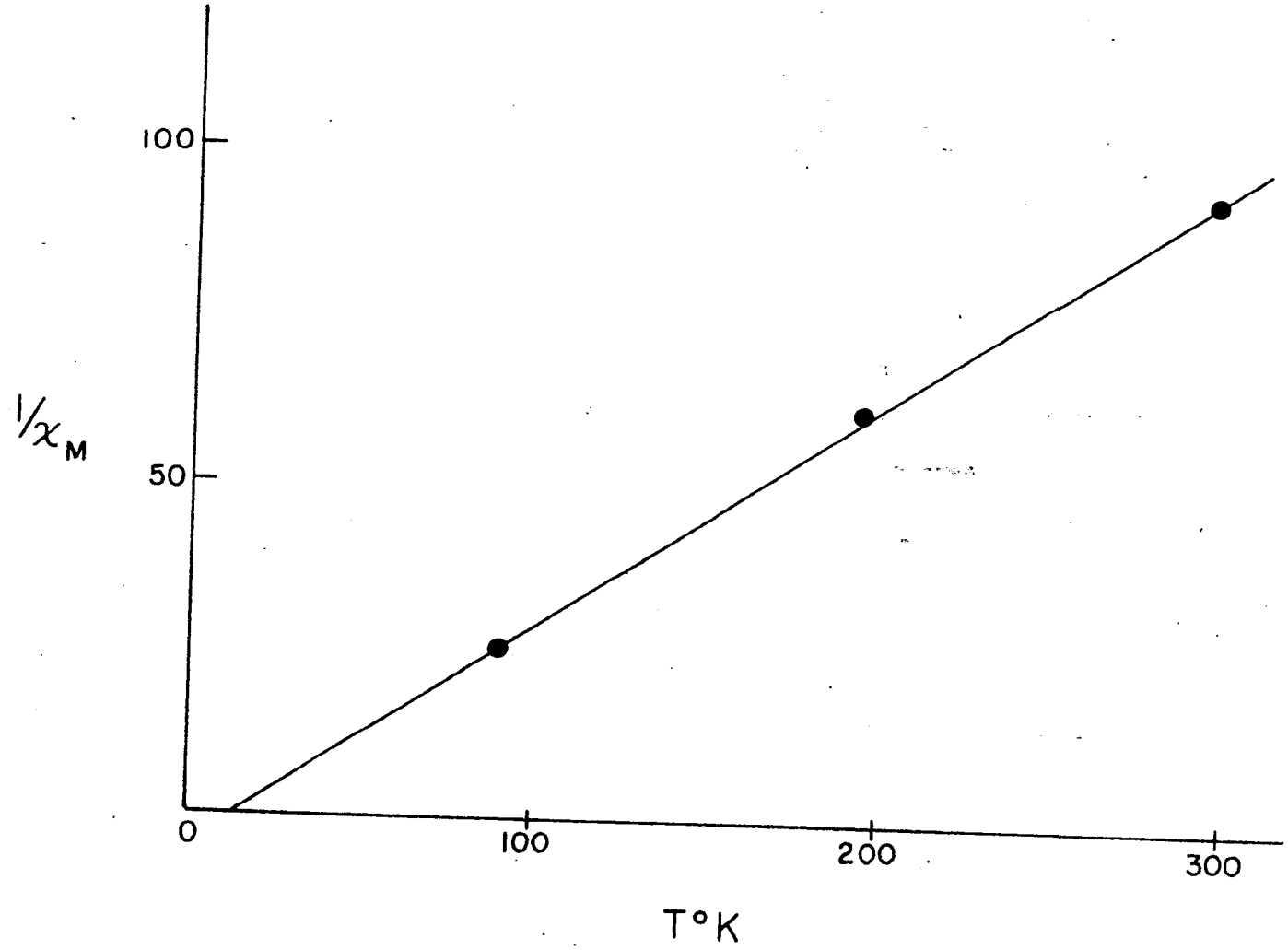
100
50
0
$1/\chi_M$
100
200
300
T°K

Figure 9. Ordering of d_{z^2} orbitals for the compound MnF_3.

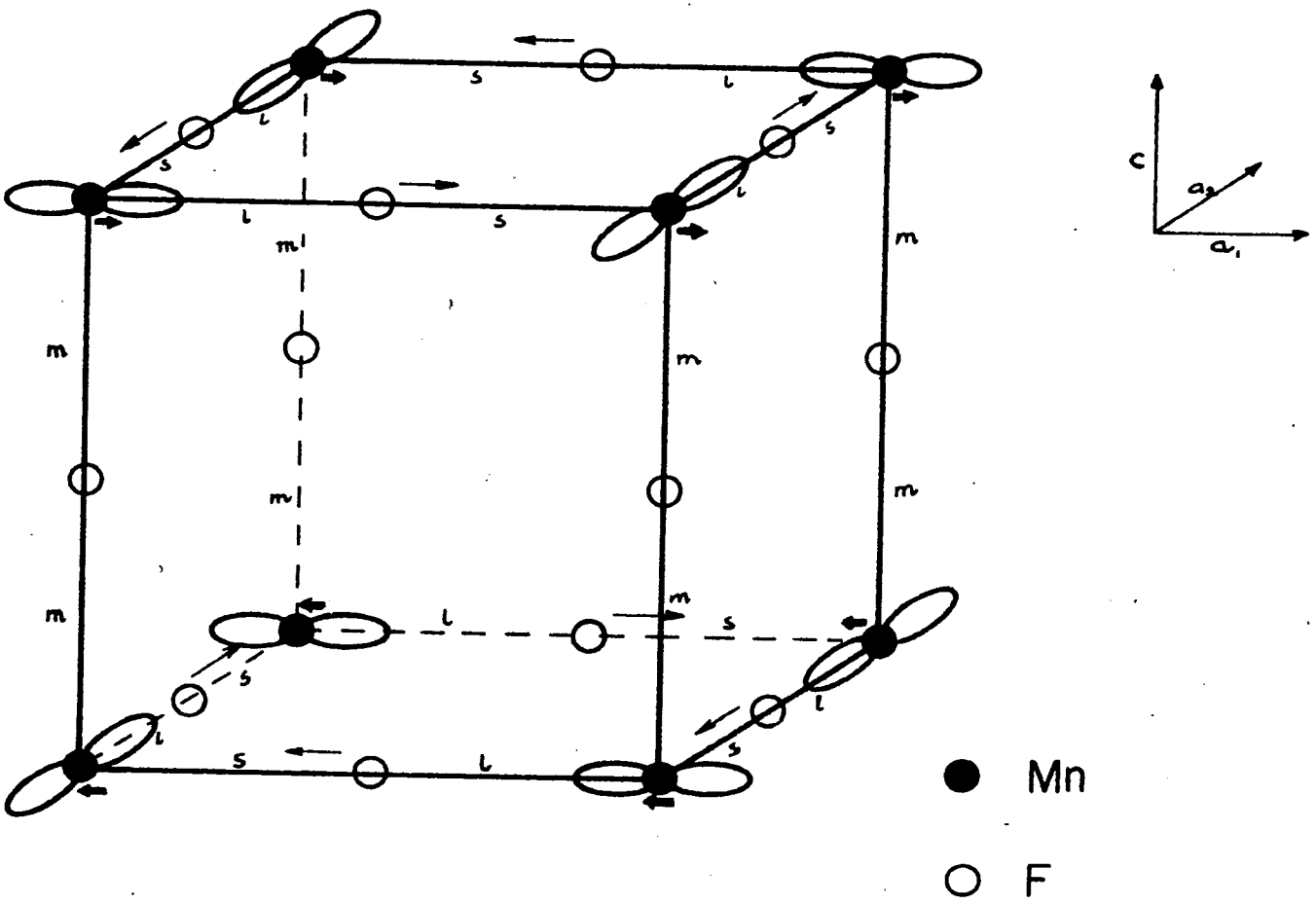
s
l
m
c
a_2
a_1
Mn
F

The magnetic structure of MnF_3 is similar to that of $LaMnO_3$ previously observed by E.O. Wollan.[45] This structure appears to be associated with the presence of only one electron in the e_g orbitals. In a cation with a $3d^4$ outer configuration in an octahedral coordination, the e_g orbital pair will be split into a stabilized d_{z^2} orbital and a less stable $d_{x^2-y^2}$ orbital due to a distortion of the octahedron to tetragonal symmetry with $c/a > 1$. Of the two e_g orbitals, the d_{z^2} orbital is occupied causing a greater electrostatic repulsion between cation and anion along the z-axis than perpendicular to it: also, orbital overlap with the empty $d_{x^2-y^2}$ cation orbitals further stabilizes the four coplanar bonds.

The anti-ferromagnetic structure can be accounted for by the d_{z^2} orbital arrangement as shown in Fig. 9. It consists of ferromagnetic layers on a_1-a_2 plane in which the spins in alternate layers are oppositely oriented and the anti-ferromagnetism is along the c-axis. The spacial ordering of the orbitals which is required to account for this type of structure is made reasonable by X-ray measurement[24] in which an unusual occurence of three different Mn-F bond lengths has been observed (l = 2.09 A°, m = 1.91 A° and s = 1.79 A°).

The Configuration d^8 ($t_{2g}^6 e_g^2$): Nickel (II)

The NiF_2-MgF_2 system

The magnetic susceptibility and moments of NiF_2 and the solid solutions (Ni, Mg) F_2 are given in Tables XI and XII respectively.

The moment of NiF_2 calculated by using the relation $\mu = 2.83 \sqrt{\chi_M \times (T + \Delta)}$ is somewhat higher (3.60 B.M.) than that calculated from the data of Henkel and Klemm,[30] which was 3.53 B.M. The plot of $1/\chi_M$ against T in Fig. 10 is not strictly linear, but the best straight line drawn through the three points resulted in a Weiss constant of + 175° K as compared to + 160° K obtained from the susceptibility measurement of Henkel and Klemm. Bizette[46] obtained a value of Δ considerably lower, i.e. + 115.6° K. In view of these conflicting results, the study described below seemed to be in order.

The μ_{eff} values for three temperatures increase and approach one another with increasing dilution as shown in Fig. 11. The Weiss constant decreases with increasing dilution (Fig. 12). These results are expected for a substance in which there is considerable indirect exchange. However, for concentrations decreasing below about 20% NiF_2, the effective moment at 224.5° K and at room temperature drops this may be due to impurities, possibly oxide, which become significant at low Ni concentration.

Figure 10. $1/\chi_M$ vs. T for NiF_2.

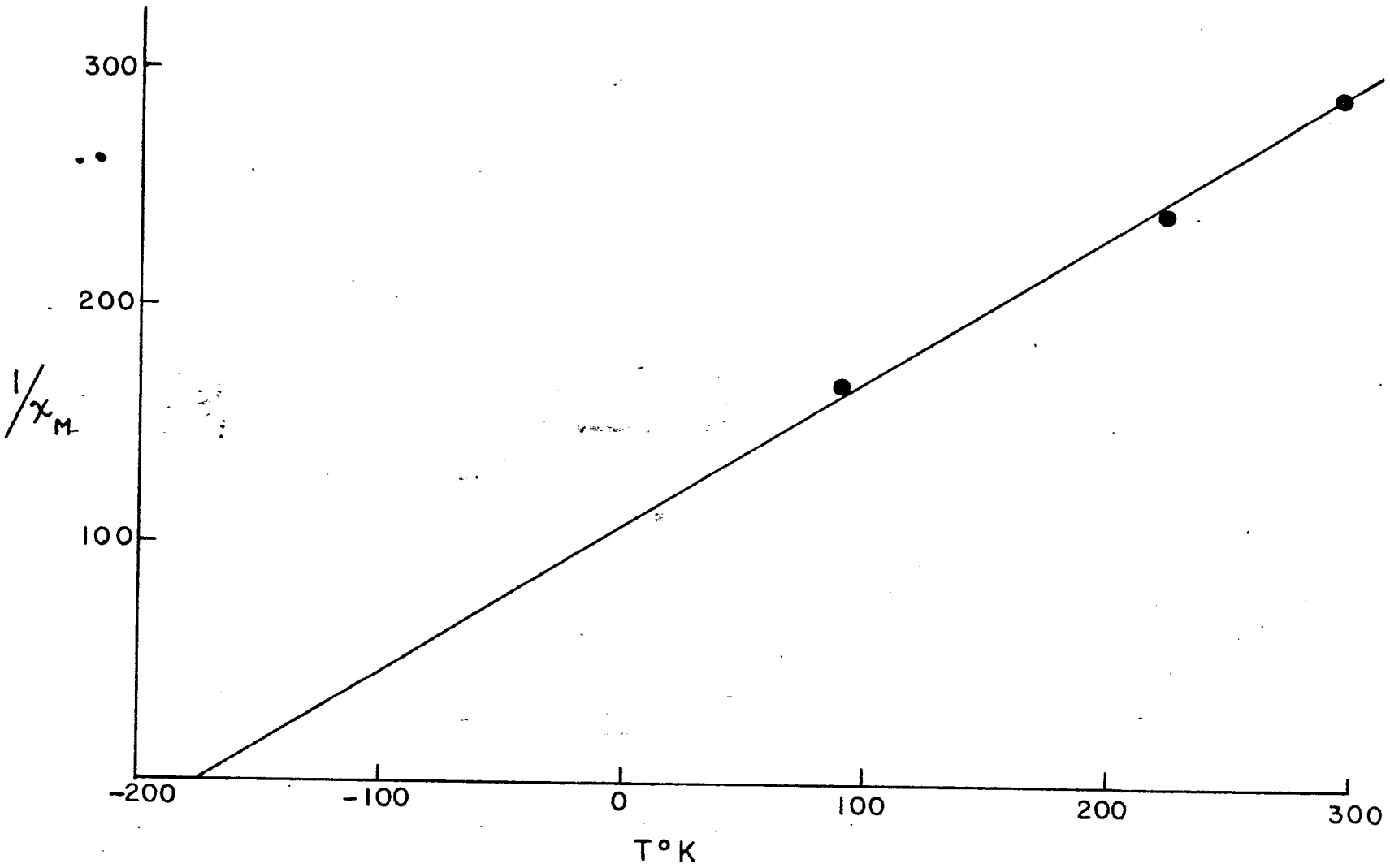
300
200
100
$1/\chi_M$
-200
-100
0
100
200
300
T°K

Figure 11. Plot of μ_{eff} vs. composition for NiF_2-MgF_2 system.

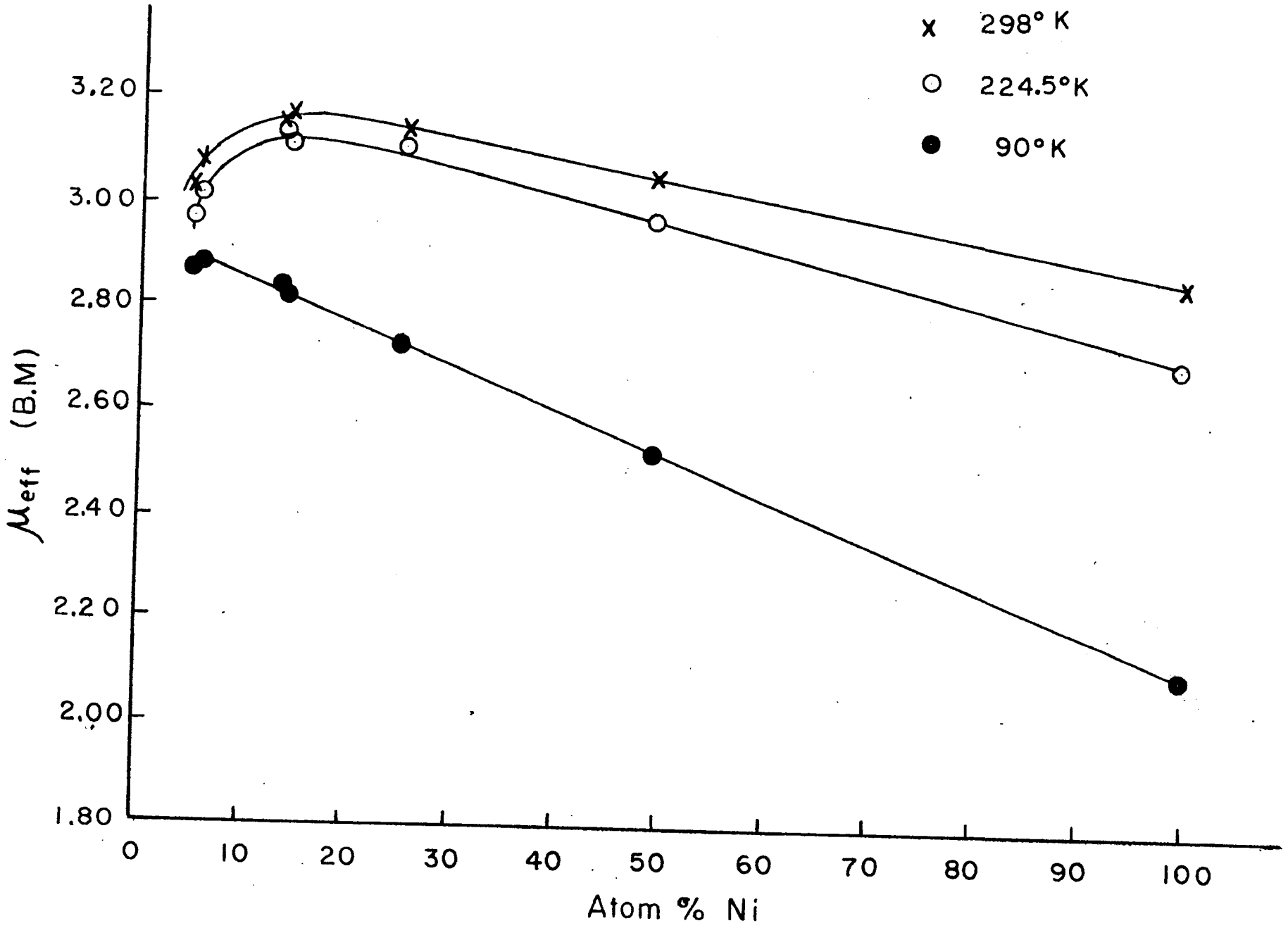
298° K
224.5°K
90°K
3.20
3.00
2.80
2.60
2.40
2.20
2.00
1.80
μ_{eff} (B.M)
0
10
20
30
40
50
60
70
80
90
100
Atom % Ni

Figure 12. $1/\chi_M$ vs. T for NiF_2-MgF_2 system.

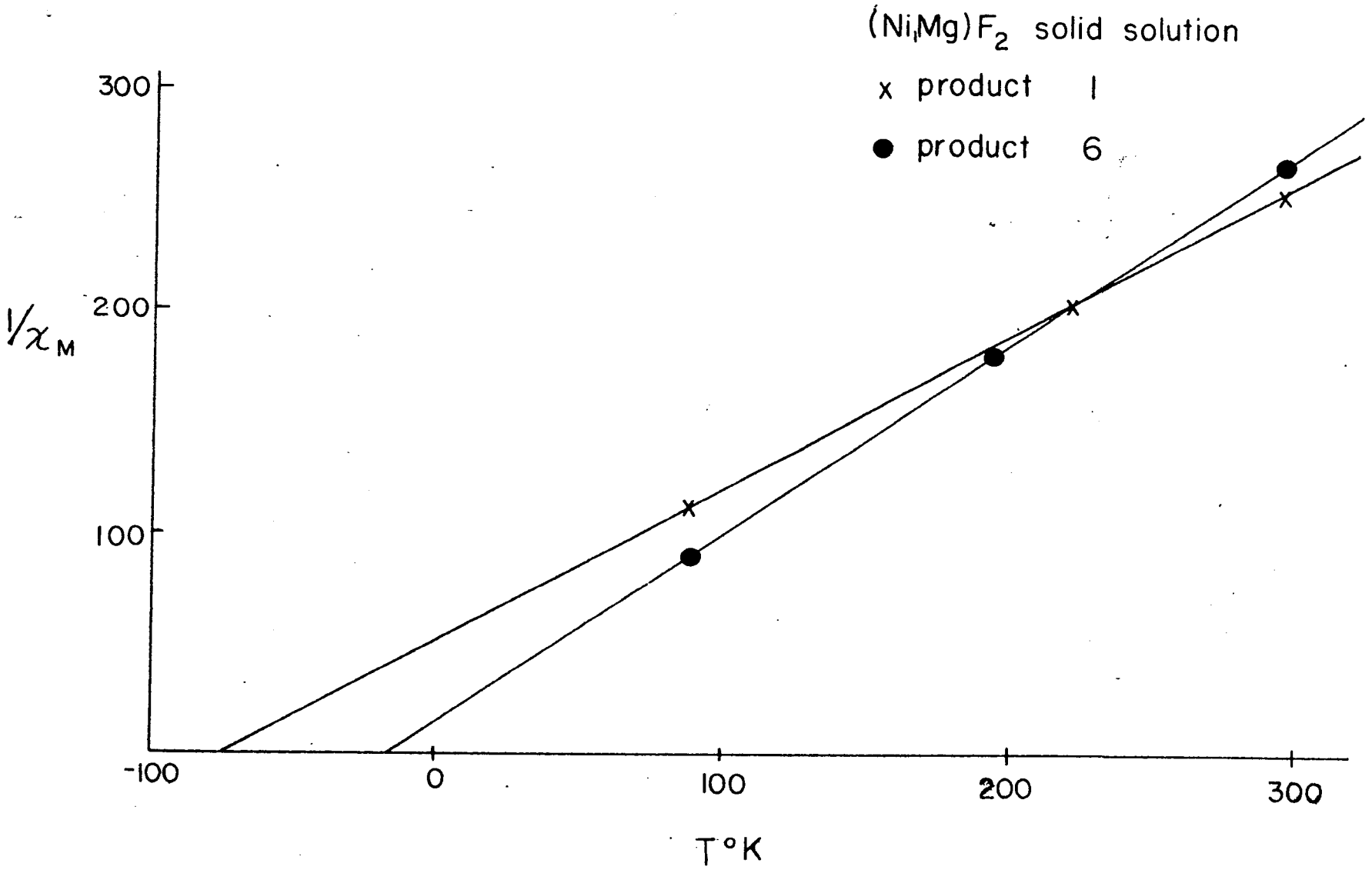
(Ni,Mg)F2 solid solution
x product 1
● product 6
300
200
100
1/χM
-100
0
100
200
300
T°K

Oxide ion in amounts up to a few percent are an almost invariable contaminant of inorganic crystalline fluorides. The introduction of an oxide ion to the coordination shell of the nickel ion can have two possible consequences:

1) An extra fluoride ion may be eliminated from the lattice.

2) The nickel ion may be raised to the triply charged state.

Table XII

Results of magnetic measurements on $(Ni,Mg)F_2$ solid solutions

Prod. No.	Temp.	$\chi_{exp} \times 10^6$	$\chi_{Ni} \times 10^3$	Δ	μ_{eff} B.M.	μ
1	298° K	24.20	3.917		3.05	3.42
	224.5° K	30.35	4.904	+75°K	2.97	3.43
	90° K	55.00	8.860		2.52	3.42
2	301.5° K	14.46	4.080		3.14	3.39
	224.5° K	19.16	5.395	+50°K	3.11	3.44
	90° K	36.76	10.320		2.72	3.40
3	298° K	8.89	4.190		3.16	3.36
	224.5° K	11.49	5.405	+39°K	3.11	3.37
	90° K	23.49	11.014		2.81	3.37

Table XII, continued

4	298° K	8.59	4.152		3.15	3.34
	224.5° K	11.29	5.446	+35°K	3.13	3.36
	90° K	23.14	11.125		2.83	3.34
5	301° K	3.718	3.925		3.08	3.17
	195° K	5.518	5.809	+20°K	3.01	3.16
	90° K	10.92	11.460		2.87	3.18
6	302.5° K	3.220	3.815		3.04	3.12
	195° K	4.790	5.658	+17°K	2.97	3.10
	90° K	9.72	11.447		2.87	3.12

An estimate of the energy to bring about these two conditions as represented by the arrangement described in Fig. 13(B) cases 1 and 2, are calculated as follows:

Case 1

Energy involved for:

a) The omission of 1^{st} $F^{-} = + A\frac{e^2}{r}\left(1 - \frac{1}{n}\right)$.

b) The omission of 2^{nd} $F^{-} = + A\frac{e^2}{r}\left(1 - \frac{1}{n}\right) + \frac{e^2}{2.5}10^8$.

c) The insertion of one $O^{=} = - A\frac{2e^2}{r}\left(1 - \frac{1}{n}\right) - \frac{2e^2}{2.5}10^8$.

$$\text{Total} = - \frac{e^2}{2.5}10^8 = - 0.4\ e^2\ 10^8 = -5.77 \text{ e.v.}$$

Figure 13. Possible oxide impurity defect structure in NiF_2.

(A)

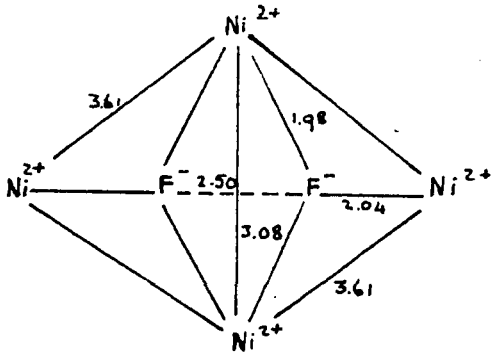

(B)

Case 1

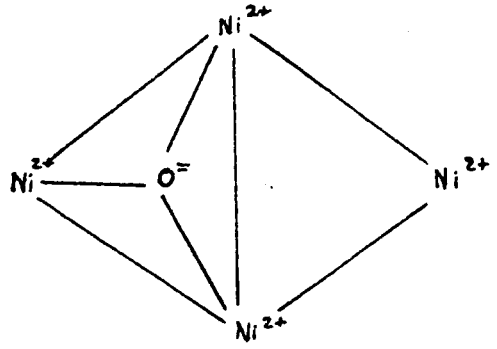

Case 2

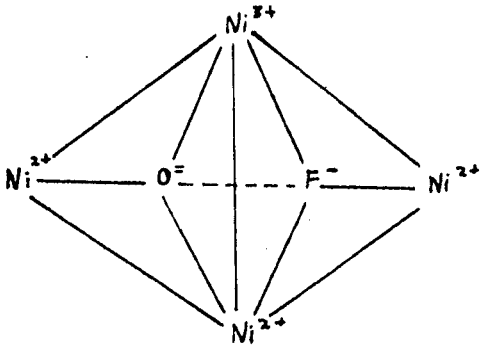

Case 2

a) The omission of one F^- = $+ A\frac{e^2}{r}(1 - \frac{1}{n})$

b) The insertion of one $O^=$ = $- A\frac{2e^2}{r}(1 - \frac{1}{n})$

c) The omission of one Ni^{2+} = $(+ A\frac{4e^2}{r} - \frac{2e^2}{r} + 4\frac{e^2}{r})(1 - \frac{1}{n})$

d) The insertion of one Ni^{3+} = $(- A\frac{6e^2}{r} + 3\frac{e^2}{r} - 6\frac{e^2}{r})(1 - \frac{1}{n})$

Total = $(-3A\frac{e^2}{r} - \frac{e^2}{r})(1 - \frac{1}{n}) = -2.04\ e^2\ 10^8$

$= -29.10$ e.v.

Here A = Madelung constant = 1.204 for a rutile type structure

r = Ni-F distance $\sim 2.01 \times 10^{-8}$ cm.

e = electron charge = 4.802×10^{-10} e.s.u.

n = Born exponent = 8.

Case (1) has also the (E - 1/2 D) energy term which amounts to 64.5 kcal/mole = 2.80 e.v. to its disadvantage. Overall energy involved in case (1) = (- 5.77 + 2.80) e.v.

$= - 2.97$ e.v.

The crystal field stabilization energy is of the same order for both Ni^{2+} and Ni^{3+} ions. The difference between case 2 and case 1 is - 26.13 e.v. which accounts for approximately 75% of the third ionization energy of nickel which is 35.16 e.v.

In the above approximation, the distortion around the Ni^{3+} and some degree of polarization of the bonds were not considered.

A similar calculation on $[AlF_6]^{3-}$ considering the fluoride ions as point charges resulted in an energy approximately 28% lower than the experimental value.[47] Thus, the value of 26.13 e.v. for the defect energy in $Ni(O,F_2)$ may be low by 9 e.v.

If a Ni^{3+} ion were to take part in the sequence Ni^{3+}-F^--Ni^{2+}, the p-orbital of the fluorine atom would overlap with a half filled e_g orbital on the Ni^{2+} ion but may overlap a vacant e_g orbital on the Ni^{3+} ion. If there is random ordering of the nickel ions of unequal charge we have Zener's condition for ferromagnetism. Such is the case with nickel fluoride which contains oxygen.

Due to the mobility of the oxide ion and the lowest energy obtained by placing the oxide ion next to a Ni^{3+} ion, it is reasonable to assume that the oxide ion migrates toward the oxidizable cation in mixed crystals of NiF_2 and MgF_2. If, as an illustration, one considers the NiF_2-MgF_2 system containing 5 mole % NiF_2, the presence of 1% oxygen impurity could result in the formation of $Ni^{II}_{0.04}$ $Ni^{III}_{0.01}$ $Mg_{0.95}$ $F_{1.99}$ $O_{0.01}$ in which 20% of the nickel is present in the trivalent state. Consequently the effect of small traces of oxygen can have a pronounced effect upon the paramagnetism at high dilution.

In an attempt to demonstrate the presence of Ni (III)

ion in the present preparation, the author compared the reflection spectra of a 50 mole % sample and a 5 mole % sample of NiF_2 and K_3NiF_6. These are shown in Fig. 14 and designated, (a), (b), (c), (d), respectively. The minimum absorption which occurs at approximately 600 mμ in (a) has shifted toward lower wavelengths in (b) and even more so in (c) and this approaches the corresponding one in the spectrum of K_3NiF_6 at 450 mμ in (d). Also the relative heights of the bands at 400 and 800 mμ in (c) as compared to (a) give an indication of the presence of nickel in its trivalent state.

The presence of Ni (III) should lower the average gram atomic susceptibility of the nickel fluoride as the susceptibility of the Ni (III) ion in K_3NiF_6 has been shown[29] to be lower than that of Ni (II) ion in the NiF_2-MgF_2 solid solutions of medium concentration.

If the straight line portions of the curves be extrapolated to infinite dilution, different values of the moment are obtained for different temperatures (3.23, 3.20 and 2.94 B.M. at room temperature, 224.5° K and 90° K respectively). This temperature dependence is roughly in accord with theory which takes account of spin orbit coupling in the first excited state of Ni (II) ion, i.e., the $t_{2g}^5\ e_g^3$, configuration.[48]

The moments obtained from the Curie-Weiss expression are plotted against composition in Fig. 15. The drop at low

Figure 14. Reflection spectra of

(a) NiF_2

(b) NiF_2-MgF_2 Product 1

(c) NiF_2-MgF_2 Product 6

(d) K_3NiF_6.

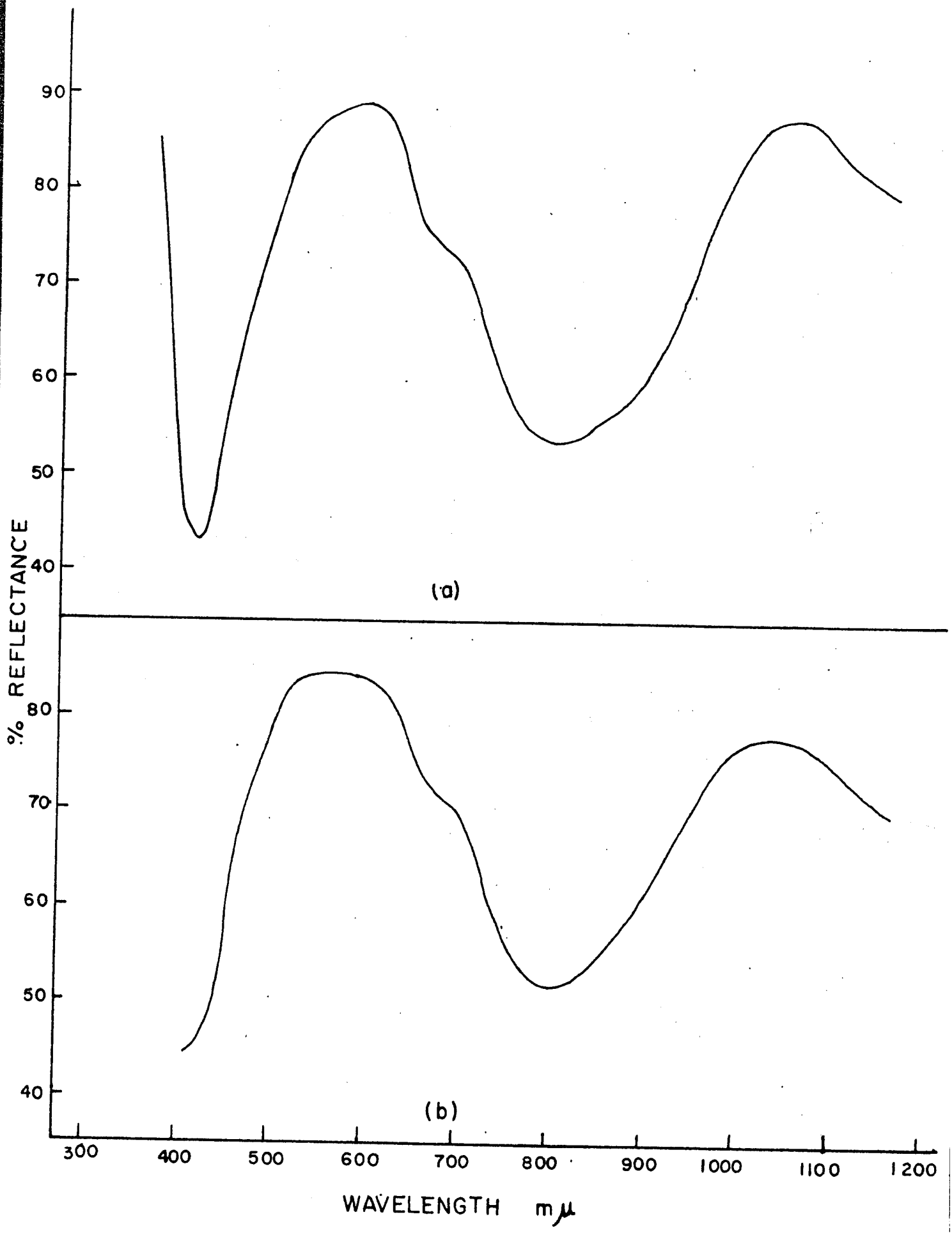
90
80
70
60
50
40
% REFLECTANCE
(a)
80
70
60
50
40
(b)
300
400
500
600
700
800
900
1000
1100
1200
WAVELENGTH mμ

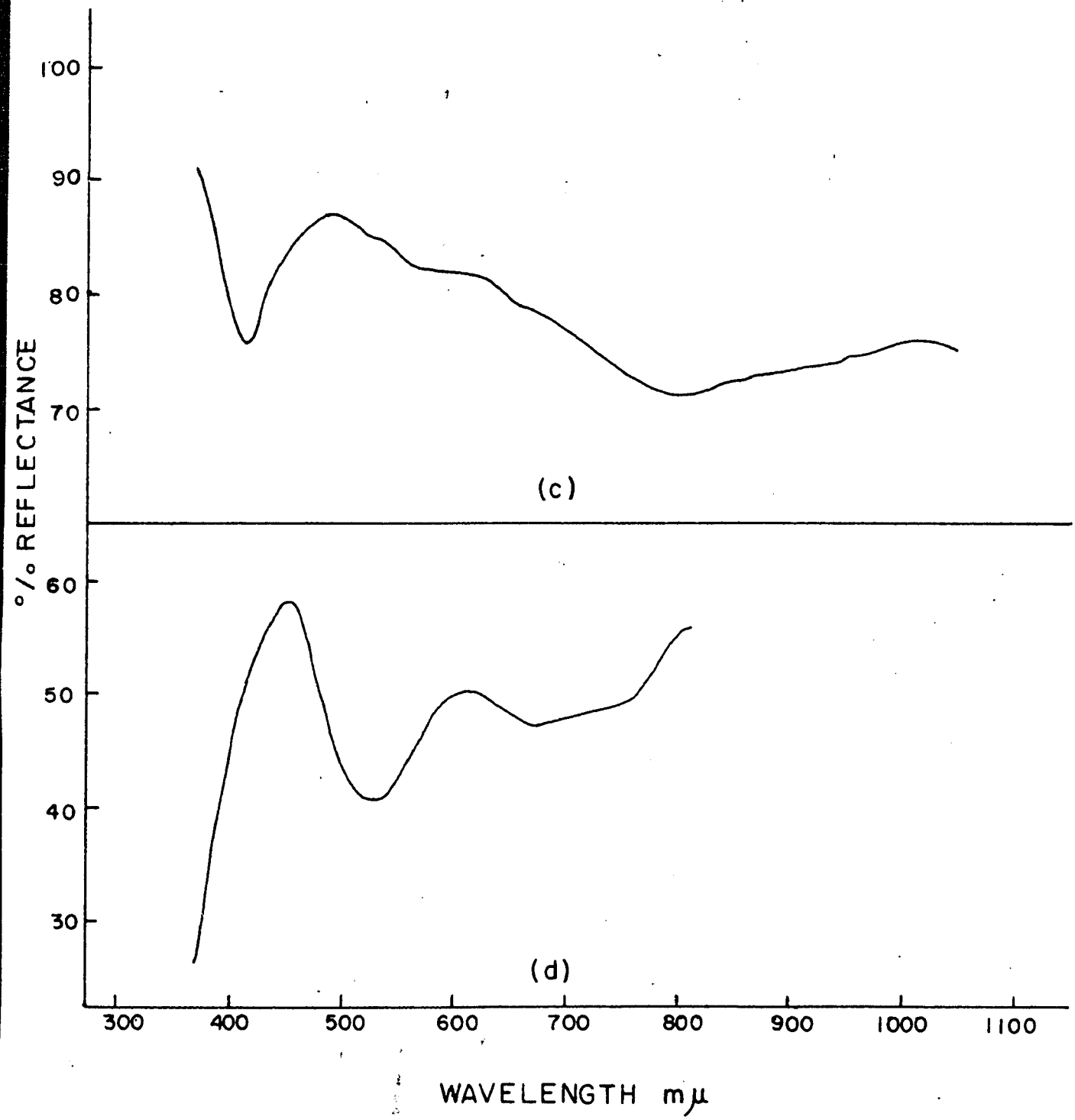
100
90
80
70
(c)
% REFLECTANCE
60
50
40
30
(d)
300
400
500
600
700
800
900
1000
1100
WAVELENGTH mμ

Figure 15. Plot of μ against composition for NiF_2-MgF_2 system.

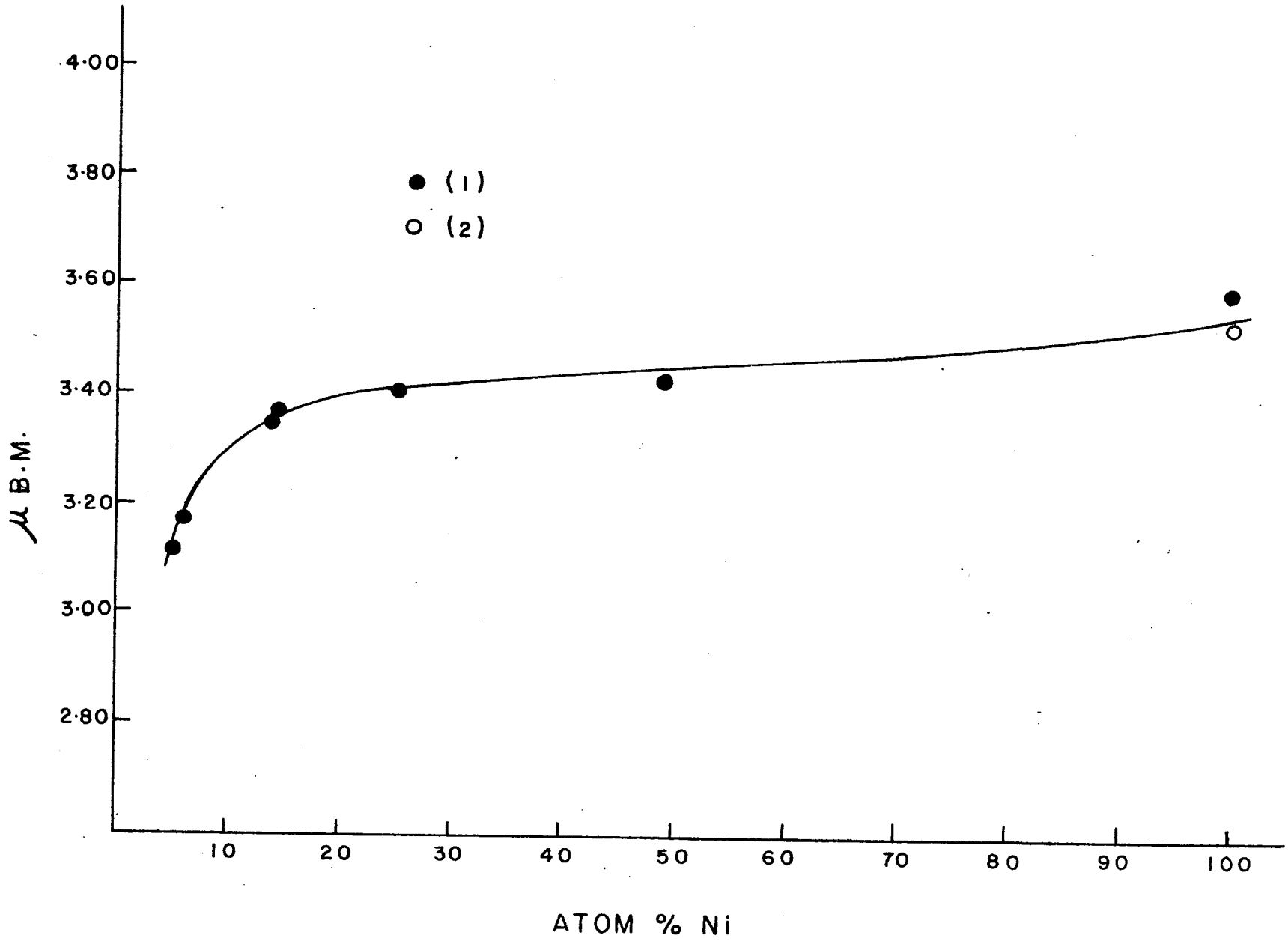
4·00
3·80
3·60
3·40
3·20
3·00
2·80
μ B.M.
● (1)
○ (2)
10
20
30
40
50
60
70
80
90
100
ATOM % Ni

Ni concentration is also attributed to the presence of oxygen impurity.

The K_2NiF_4-K_2MgF_4 System

The magnetic susceptibilities and moments of K_2NiF_4 and the solid solutions K_2NiF_4-K_2MgF_4 are given in Tables XI and XIII respectively.

The susceptibility data of K_2NiF_4 reveals a strong anti-ferromagnetism.

In K_2NiF_4, every nickel atom is surrounded octahedrally by six fluorine atoms. The NiF_6 octahedra are joined at four corners leaving two opposite corners unshared.[49] The unit cell is tetragonal, the Ni-F-Ni bond is linear, hence the compound is even more susceptible to indirect exchange than NiF_2 in which the angle is $\sim 120^{\circ}$.

Isomorphous dilution results in an increase in the effective moment as can be seen from the plot of μ_{eff} against composition in Fig. 16. Here a uniform rise of the moments with increasing dilution is shown. The large anti-ferromagnetism is overcome but again the values obtained upon extrapolation to infinite dilution are temperature dependent as is shown in Table XIV.

Figure 16. Plot of μ_{eff} against composition for K_2NiF_4 - K_2MgF_4 system.

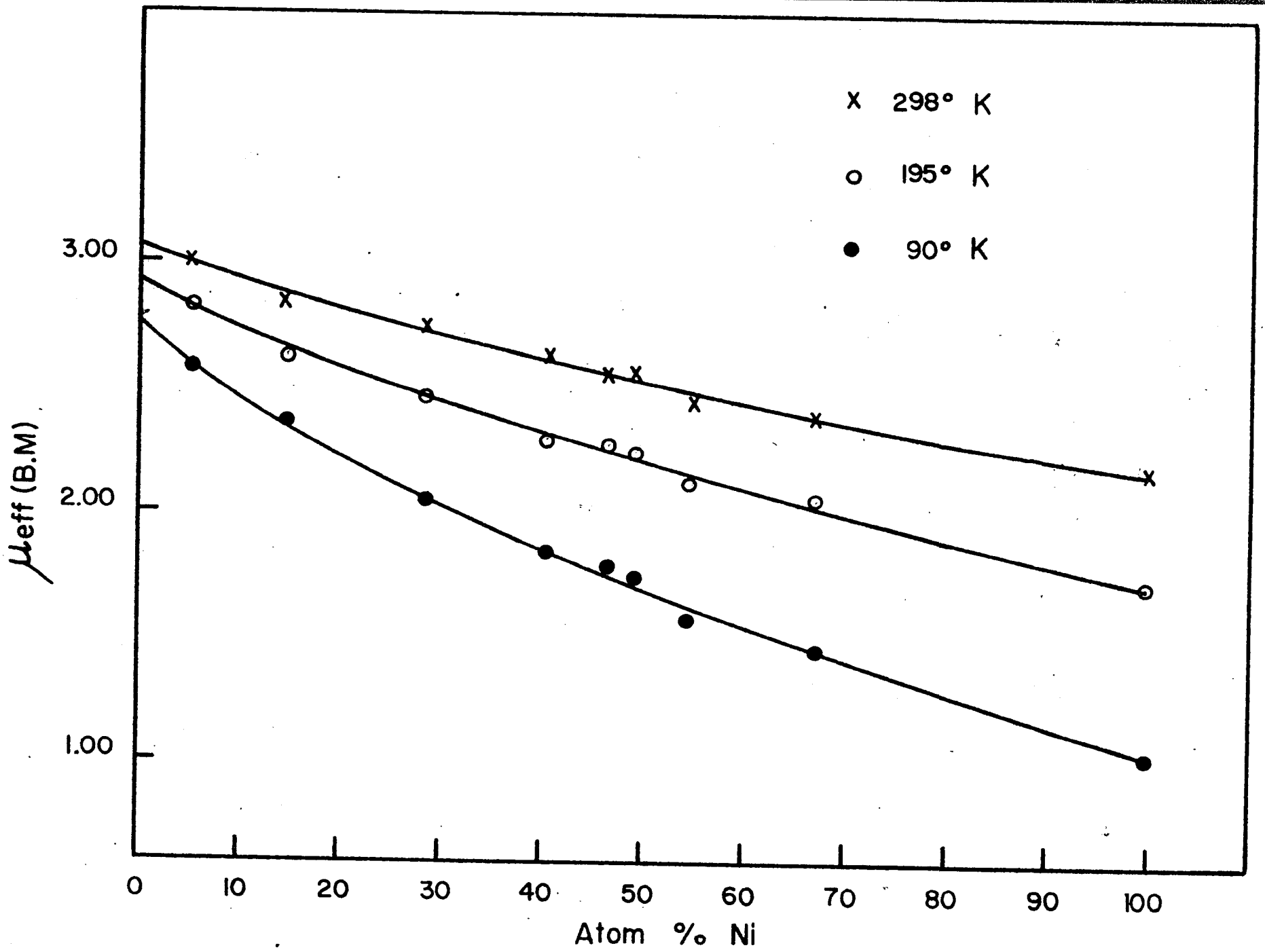
x 298° K
o 195° K
● 90° K
3.00
2.00
1.00
μeff (B.M)
0
10
20
30
40
50
60
70
80
90
100
Atom % Ni

Table XIII

Results of magnetic measurements on $K_2(Ni,Mg)F_4$ solid solutions

Prod. No.	Temp.	$\chi_{exp.} \times 10^6$	$\chi_{Ni} \times 10^3$	μ_{eff} B.M.
1	296.8° K	7.68	2.378	2.38
	195° K	8.34	2.581	2.01
	90° K	9.11	2.806	1.42
2	298° K	6.90	2.534	2.46
	195° K	7.79	2.853	2.11
	90° K	9.30	3.355	1.55
3	297° K	6.72	2.730	2.55
	195° K	7.78	3.151	2.22
	90° K	9.97	4.016	1.70
4	299° K	6.39	2.713	2.55
	195° K	7.63	3.226	2.24
	90° K	10.08	4.239	1.75

Table XIII, Continued

5	298° K	5.922	2.861	2.61
	195° K	7.02	3.379	2.30
	90° K	9.55	4.568	1.81
6	296° K	4.717	3.150	2.73
	195° K	5.842	3.884	2.46
	90° K	8.83	5.832	2.05
7	296° K	2.709	3.421	2.85
	195° K	3.523	4.427	2.63
	90° K	6.161	7.688	2.35
8	297° K	1.112	3.720	2.97
	195° K	1.512	5.032	2.80
	90° K	2.812	9.295	2.59

Table XIV

Effective moments of K_2NiF_4-K_2MgF_4 at infinite dilution

Temperature	μ_{eff} at infinite dilution
298° K	3.06 B.M
195° K	2.94 "
90° K	2.76 "

The data do not fit the Curie-Weiss law, (Fig. 17) therefore the temperature dependence is not simply due to the neglect of a Weiss constant term; rather this seems to be another instance of the temperature dependence of the orbital contribution.[48]

There is no decrease in the moments at high dilution in this system as was shown for the difluoride case. It is not clear why this case differs but it may be that the introduction of oxide ion into the lattice in this instance results in the omission of one of the singly attached fluoride ions rather than the oxidation of a Ni(II) ion to Ni(III). A similar electrostatic calculation as in the NiF_2 case has not been attempted to justify this view.

Configuration d^7, Nickel (III)

The system K_3NiF_6-$K_{2.8}AlF_{5.8}$

The effective moments of K_3NiF_6 given in Table XI are in good agreement with Hoppe's values.[29] It is difficult to prepare pure K_3NiF_6, and it was observed that the magnetic susceptibilities of K_3NiF_6 are very much affected by the presence of impurities, e.g. traces of K_2NiF_6. Since K_2NiF_6 is diamagnetic, its presence in a sample of K_3NiF_6 will decrease the susceptibility.

Figure 17. Plot of $1/\chi_M$ vs. T for K_2NiF_4-K_2MgF_4 system.

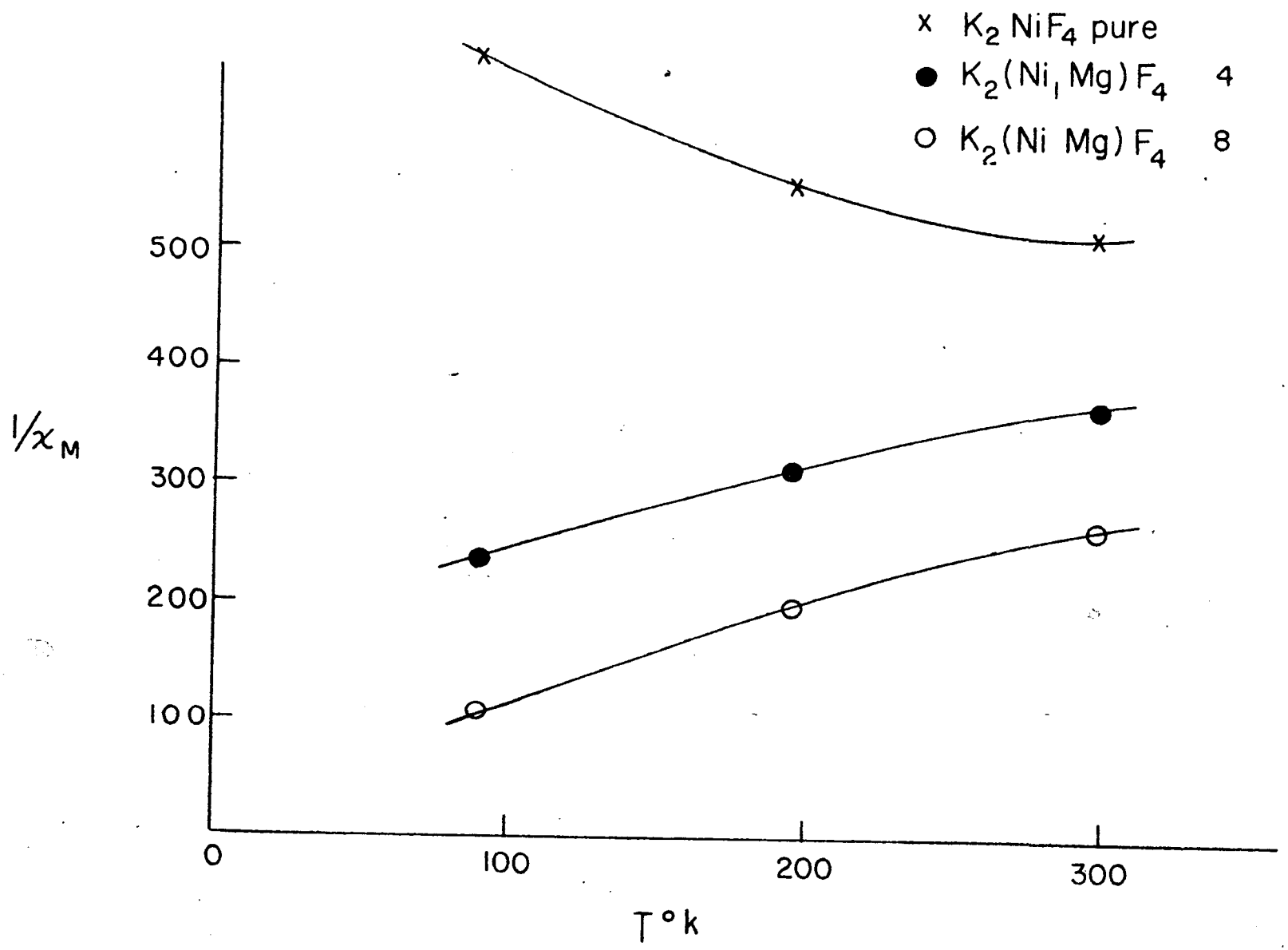
x $K_2 NiF_4$ pure
● $K_2(Ni_1 Mg)F_4$ 4
○ $K_2(Ni\ Mg)F_4$ 8
500
400
300
200
100
$1/\chi_M$
0
100
200
300
T°k

In contrast to K_3CoF_6, the effective moment of K_3NiF_6 is temperature dependent and the values are lower than the spin-only value expected for a normal complex but higher than that for a penetration complex . From the plot of $1/\chi_M$ against T in Fig. 18, it may be seen that the Curie-Weiss law is not obeyed.

Hoppe[29] suggested that K_3NiF_6, unlike K_3CoF_6 or K_3FeF_6, is not a normal complex, instead it is a case of a compound with a paramagnetic central atom in a state intermediate between a normal and a penetration complex. However, proof of this interpretation was not given. A recent paper by Klemm, Brandt and Hoppe[35] repeated the magnetic measurements on K_3NiF_6. Their results tabulated in Table XV are in good agreement with Hoppe's previous values and the present results.

Alternatively, this magnetic misbehaviour of K_3NiF_6 may be explained as being due, at least in part, to indirect exchange. But it is here suggested that fluoro complexes of iron group elements containing discrete MeF_6 octahedra are free from this interaction.

Figure 18. Plot of $1/\chi_M$ against T for K_3NiF_6-$K_{2.8}AlF_{5.8}$ system.

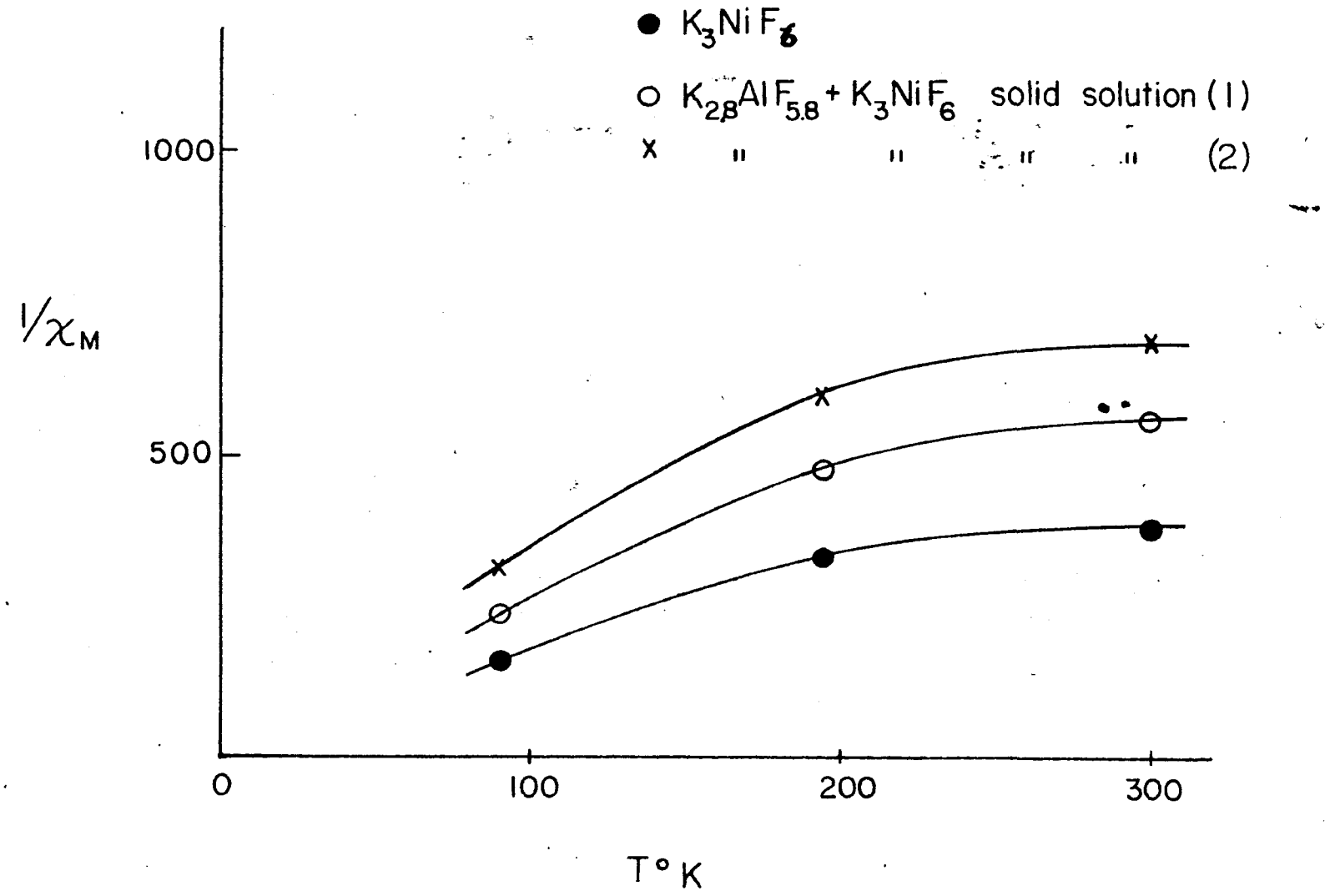
● K_3NiF_6
○ $K_{2.8}AlF_{5.8} + K_3NiF_6$ solid solution (1)
× " " " " (2)
1000
500
$1/\chi_M$
0
100
200
300
T° K

Table XV

Magnetic susceptibilities and moments of K_3NiF_6.[35]

Sample No.	Temp.	$\chi_M \times 10^6$	μ_{eff}
I	90° K	6240	2.13
	195° K	3280	2.27
	295° K	2790	2.57
II	90° K	5960	2.08
	195° K	3270	2.26
	295° K	2680	2.53

The magnetic measurements on the solid solutions of K_3NiF_6 and $K_{2.8}AlF_{5.8}$ were intended to test for the absence of magnetic interactions. The results of the experiment are given in Table XVI.

The plot of $1/\chi_M$ against temperature for K_3NiF_6 and two mixed crystal systems are shown in Fig. 18. The significant point about these plots is the fact that the departure from Curie-Weiss law behaviour is not lessened upon dilution. The fact that the susceptibility values decrease is only incidental. It is concluded from this experiment that the temperature dependence of the effective moment is not

caused by appreciable indirect exchange coupling. The original assumption of an equilibrium between "high spin" and "low spin" states seems thus to be borne out by the present results.

Table XVI

Results of magnetic measurements on the solid solutions of K_3NiF_6 and $K_{2.8}AlF_{5.8}$

Prod. No.	Temp.	$\chi_{exp} \times 10^6$	$\chi_{Ni} \times 10^3$	μ_{eff} (B.M.)
1	302° K	1.433	1.824	2.10
	195° K	1.683	2.126	1.82
	90° K	3.423	4.217	1.74
2	301° K	0.493	1.507	1.90
	195° K	0.552	1.681	1.62
	90° K	1.081	3.197	1.57

The overall decrease in the values of the susceptibility is presumed once again to be due to the presence of oxide ion in the coordination sphere of the nickel ion. In this case the Ni(IV) F_5O group would be diamagnetic and should influence the average susceptibility values even more strongly than in

the NiF_2-MgF_2 system . The diamagnetism of the quadrivalent nickel ion is exhibited in the compound K_2NiF_6.[22]

There is indication of the presence of Ni (IV) in the reflection spectrum shown in Fig. 19 (b). In this the relative heights of the bands at 530 mμ and 650 mμ and also the shoulder at approximately 400 mμ provide evidence of the presence of the higher oxidation state as may be seen by comparing the spectrum with that of K_2NiF_6 given in Fig. 19 (a).

Figure 19. Reflection spectra of

(a) K_2NiF_6

(b) K_3NiF_6-$K_{2.8}ALF_{5.8}$ product 2.

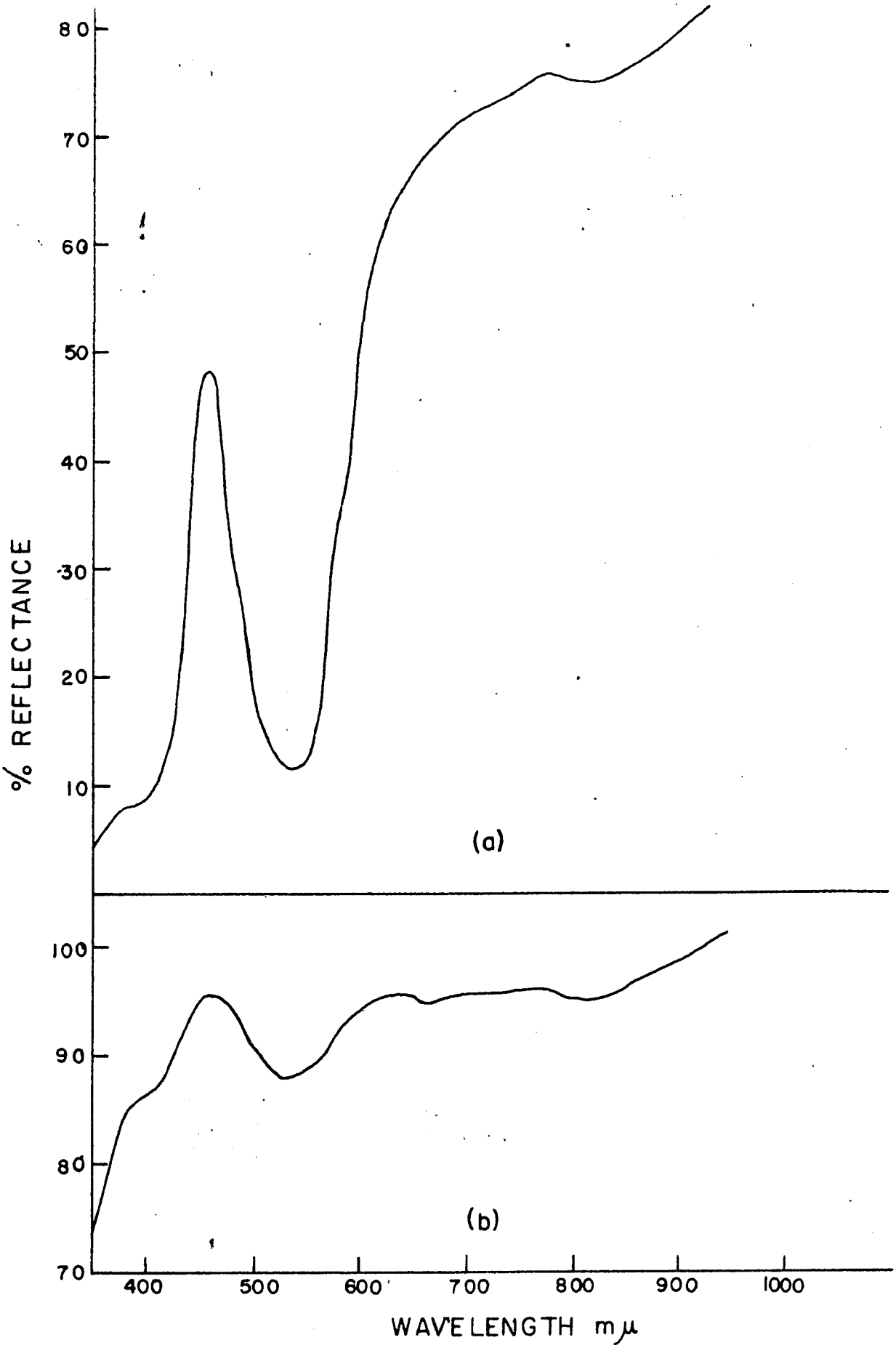
80
70
60
50
40
30
20
10
% REFLECTANCE
(a)
100
90
80
70
(b)
400
500
600
700
800
900
1000
WAVELENGTH mμ

CONCLUSIONS

Certain conclusions may be obtained from the present investigation. The assumption that fluorides and fluoro complexes, like the corresponding oxides, are magnetically concentrated was borne out by experiment. It is possible to account for the properties of these substances by assuming that magnetic interactions are of indirect type (cases (a) and (b) in Fig. 1).

Indirect exchange can occur when the anion has the proper orbital symmetry that can overlap with the paramagnetic cation orbitals in the cation-anion-cation sequence.

In NiF_2 and K_2NiF_4 this happens to be the case and strong anti-ferromagnetism is found in both compounds. This is also true for MnF_3 although the anti-ferromagnetism is overlaid by ferromagnetism. No definite conclusion can be drawn from the behaviour of VF_3, but it is possible that indirect exchange is also present in this case by the mechanism (a) in Fig. 1. Compounds of the first transition series containing discrete MeF_6, like K_3NiF_6, do not show these interactionsas expected.

It can also be concluded that the magnitude of indirect exchange in a compound is largely governed by the structure of the compound. In NiF_2 both of the unpaired e_g electrons of

Ni(II) participate in the indirect coupling, but only one of the two in the case of K_2NiF_4, yet anti-ferromagnetism in K_2NiF_4 is greater than in NiF_2. This is attributed to the more favourable structure of K_2NiF_4 in which the Ni-F-Ni bond is linear as compared to the non-linear Ni-F-Ni bond in NiF_2. This is also observed in CrF_3. The e_g orbital pair is unfilled in Cr(III) with octahedral environment, therefore the exchange interaction might be expected to be relatively small. However, the anti-ferromagnetism is pronounced in the case of trifluoride. This is again due to the favourable structure of CrF_3 in which the Cr-F-Cr sequence is almost linear and the sub-lattices are joined in three dimensions.

At infinite dilution the paramagnetic Ni(II) ions exhibit an effective moment which is dependent upon temperature. This is ascribed to the temperature dependent contribution of the orbital moment of the first configurational excited state.

This leads us to the most interesting conclusion which is that of all the halides, fluorides, even when magnetically dilute, may show the largest magnetic "anomalies" rather than the opposite situation that was expected. This can be understood when it is realized that asymmetric ligand fields tend to diminish the orbital contribution which causes the magnetic moment to be dependent upon temperature. It is readily

seen that electric fields in layer lattices which are almost invariably found among paramagnetic chlorides, bromides and iodides, are far from symmetrical while the field in the corresponding fluorides which crystallize in coordination lattices are usually quite regular. Thus VF_3, NiF_2, and K_2NiF_4, show a temperature dependence of the moment even at infinite dilution as is to be expected from the most recent theories of magnetism, while chlorides, oxo-salts, etc. do not.*

The oxide impurities which are present in most fluorides probably provide a serious limitation to the technique of isomorphous dilution.

* For example, in the $NiCl_2$-$MgCl_2$ system which has been studied by A.D. Westland and R. Hoppe (unpublished work) no change in the moment of the nickel ion was observed upon dilution. The Curie-Weiss law was obeyed throughout.

REFERENCES

1. Langevin, J. de Physique (4), 4, 678 (1905); Ann. Chim. Phys. (8), 5, 70 (1905).
2. P. Curie, Ann. de Chim. et Phys., (7), 5, 289 (1895).
3. J.H. Van Vleck, The Theory of Electric and Magnetic Susceptibilities, Oxford University Press, Oxford, 1932.
4. P.W. Selwood, Magnetochemistry, Interscience Publishers, New York, 1956.
5. P. Weiss, J. Phys., 6, 661 (1907).
6. L. Néel, Ann. Phys., 18, 64 (1932); ibid. 5, 256 (1936).
7. L. Néel, Ann. Phys., 3, 137 (1948).
8. H.A. Kramers, Physica, 1, 182 (1934).
9. E. Huthén, Proc. Amsterdam Acad. Sci., 39, 190 (1936).
10. F. Bitter, Phys. Rev., 54, 79 (1938).
11. J.H. Van Vleck, J. Chem. Phys., 9, 85 (1941).
12. J.H. Van Vleck, Colloques Internationaux, Ferromagnetism and Anti-ferromagnetism, Grenoble, 1950, p. 114.
13. C. Zener, Phys. Rev., 82, 403 (1951).
14. J.B. Goodenough and A.L. Loeb, Phys. Rev., Vo. 98, 2, 391-408 (1955).
15. J.S. Griffith and L.E. Orgel, Quart. Rev., XI, 381-93 (1957).
16. H. Bethe, Ann. Phys., 3, 133 (1929).

17. R. Schlapp and W.G. Penney, Phys. Rev., 42, 666 (1932).

18. C.K. Jorgensen, Proceedings 10th. Solvay Congress, Brussels, 1956.

19. L.E. Orgel, J. Chem. Phys., 23, 1004 (1955).

20. J.H. Van Vleck, J. Chem. Phys., 3, 803 and 807 (1935).

21. K.D. Bowers and J. Owen, Reports Progr. Phys., 18, 304 (1955).

22. R.S. Nyholm and A.G. Sharpe, J.C.S., 3579 (1952).

23. H. Bizette and B. Tsai, Compt. rend., 211, 252-53 (1940).

24. M.A. Hepworth, K.H. Jack and R.S. Nyholm, Nature, 179, 211 (1957).

25. R.L. Martin, R.S. Nyholm and N.C. Stephenson, Chem. and Industry, 83 (1956).

26. R.D. Peacock, Rec. Trav. Chim., 75, 576 (1956).

27. R. Hoppe and K. Blinne, Z. Anorg. und Allgem., 291, 269 (1957).

28. E. Cotton-Feytis, Ann. Chim., 4, 9 (1925).

29. R. Hoppe, Proceedings in the International Conference on Coordination Compounds, 1955.

30. P. Henkel and W. Klemm, Z. Anorg. und Allgem. Chem., 222, 70-2, (1935).

31. A.D. Westland and R. Hoppe, private communication.

32. N.C. Bhiwandker, Thesis, Univ. of Ottawa, 1960.

33. H.S. van Klooster (W. Mellor Comprehensive Treatise in Inorg. Chem. IV, p. 340).

34. R.M. Caven and W. Johnson (see W. Mellor XV, p. 469).

35. Klemm, W. Brandt and R. Hoppe, Z. Anorg. und Allgem. Chem., 308, 187 (1961).

36. H.T.S. Britton, J.C.S., 121, 982 (1922).

37. R.J. Meyer and K. Rötgers (see W. Mellor XII, p. 236).

38. R. Hoppe, private communication (see Georg Brauer, Handbuch der präparativen anorg. Chem., p. 246).

39. H.M. Spencer and J.L. Justice, J.A.C.S., 56, 2306 (1934).

40. D.E. Carpenter et al, U.S., 2, 743, 161 (1956).

41. E.O. Wollan, H.R. Child, W.C. Koehler, and M.K. Wilkinson, Phys. Rev., 112, 1132-36, (1958).

42. B.N. Figgis, Nature, 182, 1568-70 (1958).

43. K.H. Jack and V. Gutmann, Acta Crysta., 4, 246-9 (1951).

44. R.M. Bozorth and J.W. Nielsen, Phys. Rev., 110, 879-80 (1958).

45. E.O. Wollan and W.C. Koehler, Phys. Rev., 100, 545 (1955).

46. H. Bizette, Annal. Phys., 12, Vol. 1, 318-20, (1946).

47. F. Basolo and R.G. Pearson, Mechanism of Inorganic Reactions p. 48-50, 1958.

48. B.N. Figgis, Trans. Far. Soc., 57, 198, (1961).

49. D. Balz and K. Plieth, Z. Elektrochem. Angew. Phys. Chem., 59, 545 (1955).